DTIC FILE COPY

(4)

AD-A202 114

AFGL-TR-87-0324

Analysis of the Scattering and Extinction Properties of Atmospheric Particulates From the FTD Field Measurement Program

Kurt A. Kebschull
John R. Hummel

OptiMetrics, Inc
50 Mall Road
Burlington, MA 01803

20 November 1987

Scientific Report No. 4

APPROVED FOR PUBLIC RELEASE; DISTRIBUTION UNLIMITED

AIR FORCE GEOPHYSICS LABORATORY
AIR FORCE SYSTEMS COMMAND
UNITED STATES AIR FORCE
HANSCOM AIR FORCE BASE, MASSACHUSETTS 01731-5000

"This technical report has been reviewed and is approved for publication"

(Signature)
ERIC P. SHETTLE
Contract Manager

(Signature)
DONALD BEDO
Branch Chief

FOR THE COMMANDER

(Signature)
R. EARL GOOD
Acting Division Director

This report has been reviewed by the ESD Public Affairs Office (PA) and is releasable to the National Technical Information Service (NTIS).

Qualified requestors may obtain additional copies from the Defense Technical Information Center. All others should apply to the National Technical Information Service.

If your address has changed, or if you wish to be removed from the mailing list, or if the addressee is no longer employed by your organization, please notify AFGL/DAA, Hanscom AFB, MA 01731. This will assist us in maintaining a current mailing list.

Do not return copies of this report unless contractual obligations or notices on a specific document requires that it be returned.

Unclassified
SECURITY CLASSIFICATION OF THIS PAGE

REPORT DOCUMENTATION PAGE

1a. REPORT SECURITY CLASSIFICATION Unclassified	1b. RESTRICTIVE MARKINGS
2a. SECURITY CLASSIFICATION AUTHORITY	3. DISTRIBUTION/AVAILABILITY OF REPORT Approved for public release; distribution unlimited
2b. DECLASSIFICATION/DOWNGRADING SCHEDULE	
4. PERFORMING ORGANIZATION REPORT NUMBER(S) OMI-245	5. MONITORING ORGANIZATION REPORT NUMBER(S) AFGL-TR-87-0324
6a. NAME OF PERFORMING ORGANIZATION OptiMetrics, Inc. 6b. OFFICE SYMBOL (If applicable)	7a. NAME OF MONITORING ORGANIZATION Air Force Geophysics Laboratory
6c. ADDRESS (City, State, and ZIP Code) 50 Mall Road Burlington, MA 01803	7b. ADDRESS (City, State, and ZIP Code) Hanscom AFB, MA 01731
8a. NAME OF FUNDING/SPONSORING ORGANIZATION Air Force Geophysics Lab 8b. OFFICE SYMBOL (If applicable) OPA	9. PROCUREMENT INSTRUMENT IDENTIFICATION NUMBER F19628-85-C-0178
8c. ADDRESS (City, State, and ZIP Code) Hanscom AFB, MA 01731	10. SOURCE OF FUNDING NUMBERS PROGRAM ELEMENT NO: 62101F PROJECT NO: 7670 TASK NO.: 15 WORK UNIT ACCESSION NO: AI

11. TITLE (Include Security Classification)
Analysis of the Scattering and Extinction Properties of Atmospheric Particulates From the FTD Field Measurement Program

12. PERSONAL AUTHOR(S)
Kurt A. Kebschull and John R. Hummel

13a. TYPE OF REPORT	13b. TIME COVERED	14. DATE OF REPORT (Year, Month, Day)	15. PAGE COUNT
Scientific Report #4	FROM 4/87 TO 11/87	87 November 20	76

16. SUPPLEMENTARY NOTATION

17. COSATI CODES			18. SUBJECT TERMS (Continue on reverse if necessary and identify by block number)
FIELD	GROUP	SUB-GROUP	Atmospheric Aerosols, Abridged Polar Nephelometer (APN), Transmission, TSCF, FTD Field Measurements, Aerosol Scattering and Extinction

19. ABSTRACT (Continue on reverse if necessary and identify by block number)

Field test measurements related to the scattering and extinction properties of atmospheric particulates have been reviewed, validated and analyzed. The data were taken between 6-10 October 1986 at the Targeting Systems Characterization Facility at Wright-Patterson AFB, Ohio. The data taken include routine Air Weather Service surface observations, meteorological measurements, transmission measurements from the continuously variable filter transmissometer, visual quality, visual range, aerosol concentrations and aerosol scattering from the abridged polar nephelometer (APN).

The review of the data revealed some problems and inconsistencies that made a complete analysis difficult. This was especially true in the IR transmission and APN data. No explanation can be given for the inconsistencies in the transmission data. The problems in the APN data are believed to be due to calibration problems in the instrument.

20. DISTRIBUTION/AVAILABILITY OF ABSTRACT ☐ UNCLASSIFIED/UNLIMITED ☐ SAME AS RPT ☐ DTIC USERS	21. ABSTRACT SECURITY CLASSIFICATION Unclassified
22a. NAME OF RESPONSIBLE INDIVIDUAL Eric P. Shettle	22b. TELEPHONE (Include Area Code) 617-377-3665 22c. OFFICE SYMBOL OPA

DD FORM 1473, 84 MAR — 83 APR edition may be used until exhausted. All other editions are obsolete.

SECURITY CLASSIFICATION OF THIS PAGE

Table of Contents

Illustrations

Tables

1. INTRODUCTION

This report reviews and analyzes data taken during a field measurement program that was conducted at the Targeting Systems Characterization Facility (TSCF), Wright-Patterson Air Force Base, Ohio between 6-10 October 1986. The data were taken in support of programs conducted by the Foreign Technology Division (FTD). The report comments on the completeness, quality and consistency of the data, as well as the significance of variations in the various parameters.

1.1 Organization of Report

Section 2 describes the test instrumentation and data that were taken during the tests, focusing on the temporal extent and quality of the data. Section 3 presents comparisons of the data. Finally, Section 4 presents a summary of the results and conclusions that can be drawn from the data.

2. DESCRIPTION OF THE TEST AND INSTRUMENTATION USED

2.1 Test Location

This test was conducted at a deactivated airstrip on "Area B" of Wright-Patterson Air Force Base located north-east of Dayton, Ohio. Area B is situated on the edge of a semi-urban area with major housing areas to the northwest, west and southwest. The rest of the surrounding land is farmland or is under development. The topography of the region is best illustrated by reviewing the map in Figure 1. Basically, the elevation falls from southeast-to-northwest as one approaches the valley and flood plain of the Mad River, located approximately 2.1 km northwest of the test site. Naturally, the airfield and the test area are very flat, with gentler slopes. The landing strips are coated with asphalt, while adjacent taxiway surfaces are concrete.

The TSCF maintains a target and environmental measurement site on Area B just north of the southernmost deactivated landing strip. This area is near a U.S. Geological Survey (USGS) benchmark, indicated by "BM" in Figure 1. Instruments and targets were positioned by means of polar coordinates from this benchmark located at 39°46'34"N, 84°06'32"W, at an elevation of 795 feet (242 meters) above sea level.

Supporting environmental data were collected using the Environmental Monitoring and Control System (EMACS). Table 1 lists the parameters that were measured during the tests and also some information about the instrumentation that was

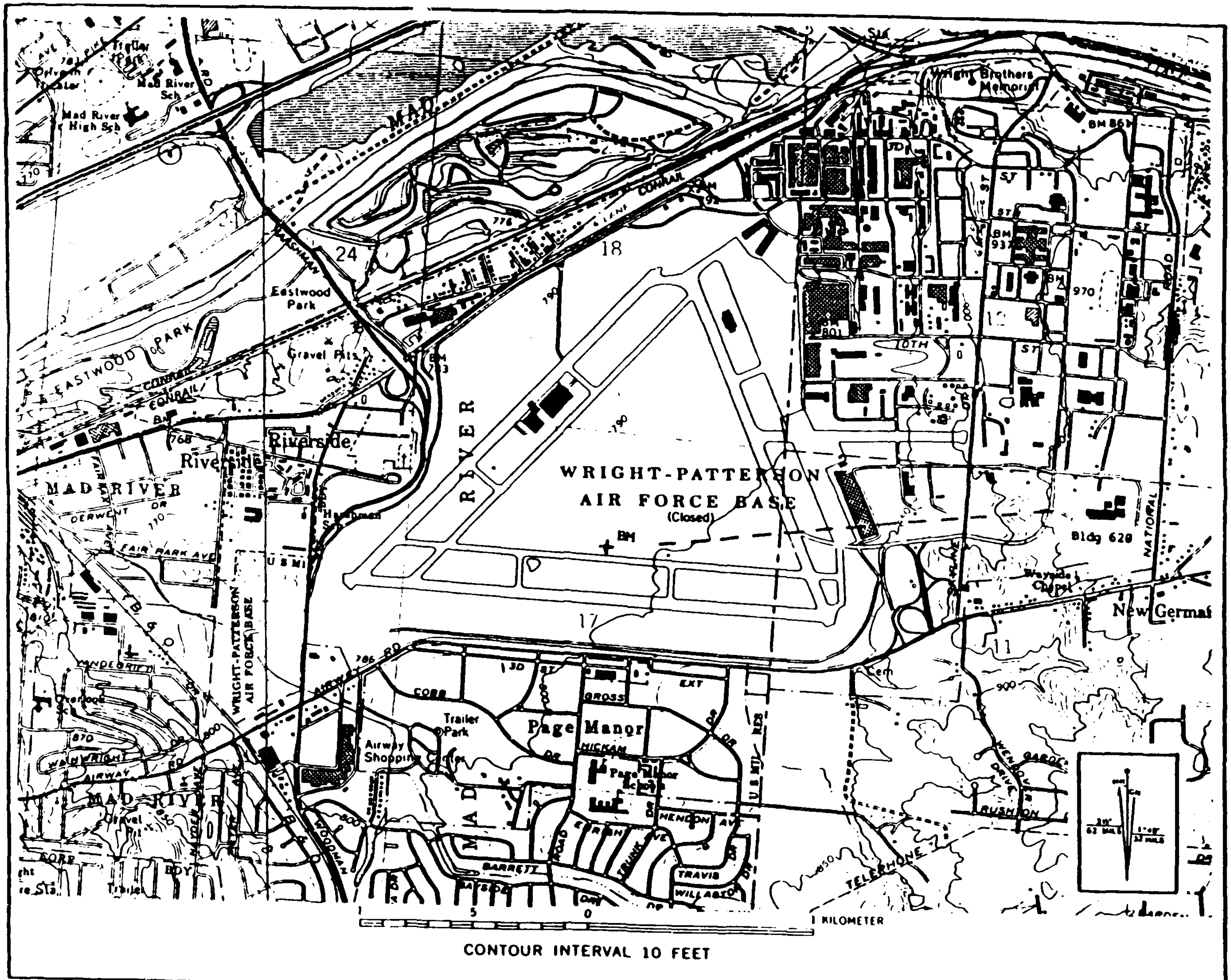

Figure 1. Map of Wright-Patterson AFB Area B and Surroundings

Table 1. Parameters Measured and Instrumentation from the EMACS Used During the FTD Field Measurement Program, 6-10 October 1986

PARAMETER	INSTRUMENTATION	UNITS	RANGE	ACCURACY
Transmission	Transmissometer Operated at Targeting Systems Characterization Facility	--		
Angular Particulate Scattering	AFGL Abridged Polar Nephelometer	km^{-1} sr^{-1}		
Air & Dew Point Temperature	EG&G 220 Temp Set	C	-50 to 50 C	+/- 1 C (T) +/- 0.4 C (DP)
Air Pressure	Weathertronics 7105-A	mb	600 - 1100 mb	0.08 %
Wind Speed	R. M. Young 35003	knots	0.4 - 87 kt	+/- 0.13 kts
Wind Direction	R. M. Young 21281	degrees	0 - 360 deg	< 1 deg
Precipitation	Weathertronics 6021A Tipping Bucket	mm	0.01 "/hr	0.0003"/pulse
Visual Quality	MRI 1550 B Integrating Nephelometer	km^{-1}	0.01 - 10 km^{-1}	+/- 10 % of range
Visual Range	Wright & Wright FOG-15	km^{-1}	0.01 - 100 km^{-1}	Variable
Visible Global Solar Radiation	Eppley PSP Pyranometer (0.3 to 3.0 μm window)	$W\ m^{-2}$	0 - 2800 $W\ m^{-2}$	+/- 0.5 %
Long Wavelength Atmospheric Radiation	Eppley PIR Pyrgeometer (3.0 to 50 μm window)	$W\ m^{-2}$	0 - 700 $W\ m^{-2}$	+/- 1 %
Aerosol Number Density	Particle Measuring Systems	# $cm^{-3} \mu m^{-1}$		

used. Additional parameters, such as absolute and relative humidity, were then calculated from the measured data. Figure 2 shows the availability of the data for each day of the test.

2.2 INSTRUMENTATION USED

2.2.1 Meteorological Measurements

Meteorological data were measured using standard instrumentation and were available, with a few exceptions, every ten minutes, from 1900 local standard time (LST) on 5 October 1986 to 0700 LST on 10 October 1986. The data record consists of the 14 variables: date, time, temperature, dew point, relative humidity, absolute humidity, pressure, wind speed and direction, visual quality, visual range, visible solar radiation, longwave atmospheric radiation and amount of precipitation. The data appear to be reasonable, with the exception of an occasional spike in the temperature and dew point temperature data that were caused by calibration routines. The original temperature and dew point data set did not always recover properly after calibration, so a replacement temperature and dew point data set was provided. The information in the replacement data set appeared to recover properly after the calibration routines were applied. It is assumed that the replacement data were taken by the same type of instrumentation as the original data set.

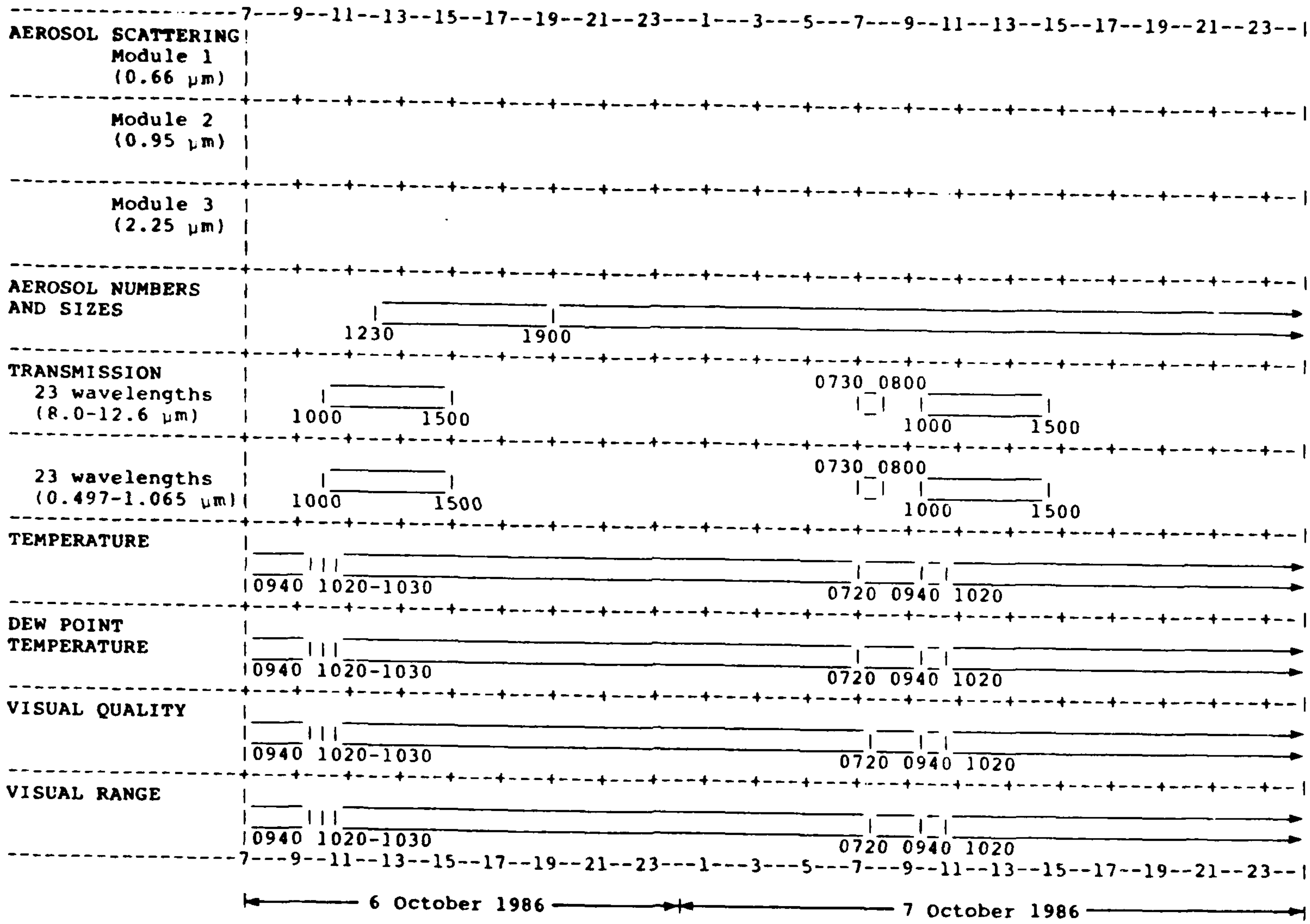

Figure 2. Operating Times, in LST, for the Instrumentation

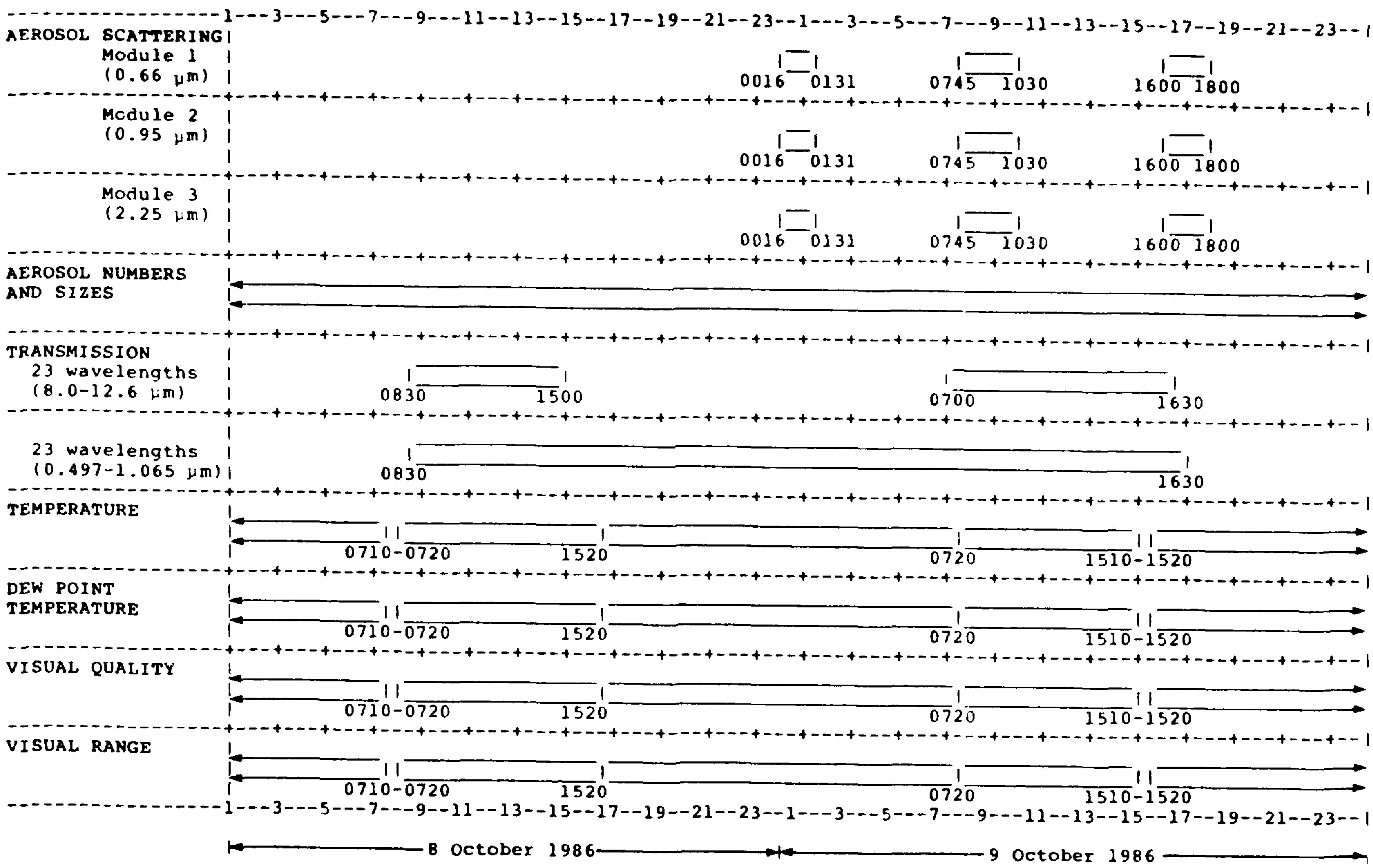

Figure 2. Operating Times, in LST, for the Instrumentation (Continued)

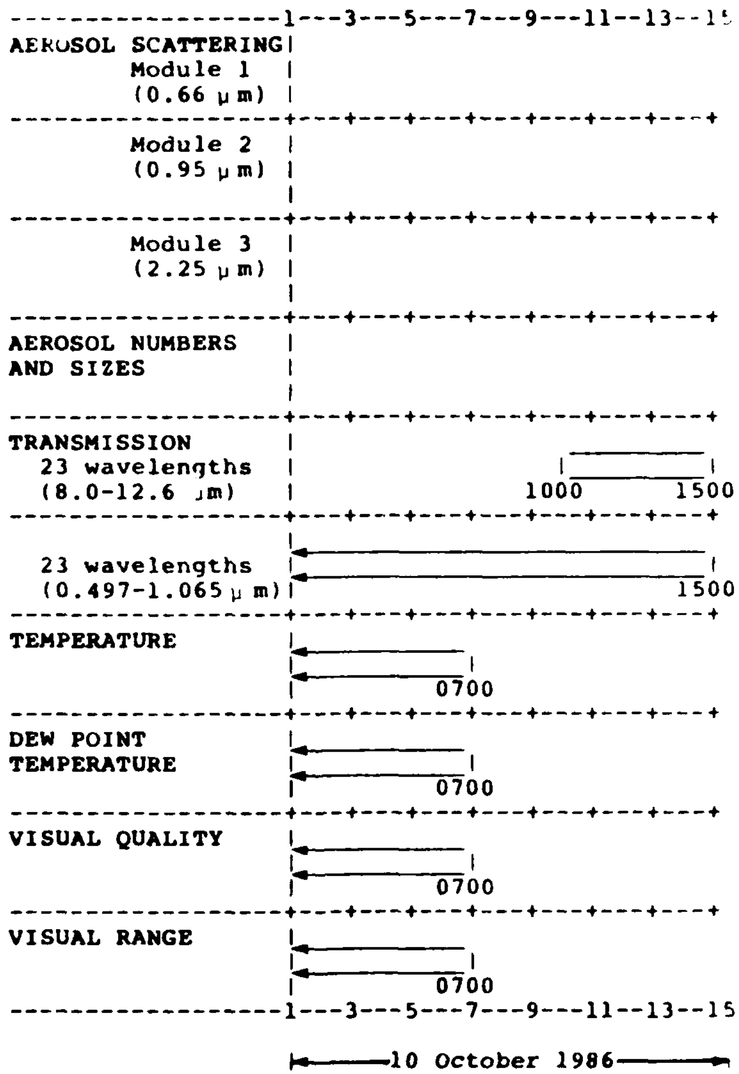

Figure 2. Operating Times, in LST, for the Instrumentation (Continued)

2.2.2 Transmission Measurements

Broadband slant-path transmission data were collected by AFWAL/AARI-3's transmissometer (eg.[1]). The transmissometer is located in the tower of Building 620. Building 620 is located to the east of the runways (see Figure 1). Data were measured over a 2.25 km path. The path was nearly horizontal with a 43 m vertical difference between end points, corresponding to a depression angle of about 2 degrees. Transmission data were available every 30 minutes on 9-10 October and partially for the days 6-8 October.

The recorded number of wavelengths varied. The instrument can make measurements over several spectral bands using a continuously variable filter wheel to step through up to 255 wavelength points. At each step, the instrument stops to sample and to average enough data to obtain a reasonable signal-to-noise ratio. Data for at least 23 wavelengths were reported at all times with an additional 23 wavelengths being reported from time to time. On a rare occasion, 150 wavelengths would be recorded, all of them being less than 1.06 μm. The first 23 wavelengths ranged from 0.497 - 0.695 microns, in increments of about 0.011 μm, and from 1.049 - 1.068 μm in steps of 0.005 μm. The second 23 wavelengths

---

1. Kneizys, F.X., Gruenzel, R.R., Martin, W.C., Schuwerk, M.J., Gallery, W.O., Clough, S.A., Chetwynd, Jr., J.H., and Shettle, E.P. (1984) Comparisons of 8 to 12 Micrometer and 3 to 5 Micrometer CVF Transmissometer Data with LOWTRAN Calculations, Air Force Geophysics Laboratory, Hanscom AFB, Massachusetts, AFGL-TR-84-0171, 26 June 1984. ADA154218

range from 7.939 to 12.652 μm, in increments of 0.214 μm. A sample data set is shown in Table 2.

2.2.3 Visual Quality Measurements

Visual quality measurements were made by a MRI integrating nephelometer. The instrument measures the atmospheric extinction due to scattering by small particles in essentially all directions.

The visual quality can be compared against the Air Weather Service (AWS) visibility observations. It is important to note that the latter are not directional visibilities, but represent the best prevailing sight distance in two quadrants. This is very different from the point measurements of scattering properties made at the test site by the visual quality instrument. Though exact correlations cannot be expected, observed visibility trends and events are often apparent in the visual quality data.

2.2.4 Visual Range Measurements

The Wright & Wright Visual Range Meter measures only forward light scattering caused by large particles, such as those of mist, drizzle, rain or snow. The data from this instrument cannot be directly compared against any other data taken by the EMACS. The data should, however, be correlated with the occurrence of phenomena that would produce the large particles that the device was designed to detect. That is, if the AWS observations reported fog or precipita-

Table 2. Representative Sample of Atmospheric Transmission Data

DATE (DMY)	TIME (GMT)	WAVELENGTH (μ m)	TRANSMISSION
61086	1500	0.497	0.853
61086	1500	0.508	0.920
61086	1500	0.518	0.963
61086	1500	0.529	0.916
61086	1500	0.540	0.931
61086	1500	0.551	0.916
61086	1500	0.563	0.892
61086	1500	0.575	0.901
61086	1500	0.587	0.912
61086	1500	0.599	0.889
61086	1500	0.611	0.903
61086	1500	0.623	0.920
61086	1500	0.635	0.898
61086	1500	0.647	0.904
61086	1500	0.659	0.905
61086	1500	0.671	0.916
61086	1500	0.683	0.900
61086	1500	0.695	0.855
61086	1500	1.049	0.672
61086	1500	1.054	0.661
61086	1500	1.059	0.658
61086	1500	1.063	0.651
61086	1500	1.068	0.654
61086	1500	7.939	0.228
61086	1500	8.153	0.550
61086	1500	8.368	0.680
61086	1500	8.582	0.713
61086	1500	8.796	0.766
61086	1500	9.010	0.786
61086	1500	9.224	0.803
61086	1500	9.439	0.790
61086	1500	9.653	0.814
61086	1500	9.867	0.832
61086	1500	10.081	0.867
61086	1500	10.296	0.866
61086	1500	10.510	0.846
61086	1500	10.724	0.866

tion, one would expect the Wright & Wright instrument to produce non-zero data.

2.2.5 Aerosol Number Density and Size Distribution Measurements

Aerosol data were taken every 20 minutes from 0530 LST on 6 October 1986 to 2100 LST on 9 October 1986. The Particle Measuring Systems (PMS) equipment utilized five sensor probes, CSASP-100, FSSP-100, OAP, OAP 2-D and GBPP. The majority of the data were recorded by the CSASP and FSSP probes. The CSASP probe covered the size range from 0.32 - 20 μm and the FSSP probe covered the range 0.50 to 47.0 μm.

The data from each probe were divided into four subranges. Each subrange was grouped into 15 bins, each subrange having the same bin width. Each subsequent subrange included larger particles with larger bin widths. The probes overlapped in the range 0.5 - 20 μm. Table 3 summarizes the size ranges and bin numbers covered by the CSASP and FSSP probes.

In some instances, particles with diameters above 47 μm were reported. These data were recorded for discrete bins; that is, no upper and lower sizes were given. These reported sizes are characteristic of cloud droplets and raindrops. However, there was no rain and little, if any, fog reported. The probes used to measure the particles with diameters above 47 μm were OAP, OAP 2-D and GBPP. The size ranges covered by these probes are, respectively, 20 - 300, 25 - 800 and 200 - 12,400 μm. Table 4 gives a sample of the aerosol data that was obtained.

Table 3. Aerosol Diameter Size Ranges and Bin Widths Used by the PMS CSASP and FSSP Probes During the FTD Field Measurements Program

BIN RANGE	SIZE RANGE (μm)	BIN WIDTH (μm)
Classical Scattering Aerosol Spectrometer Probe (CSASP)		
1 - 15	0.32 - 0.755	0.029
16 - 30	0.50 - 2.750	0.150
31 - 45	1.00 - 12.250	0.750
46 - 60	2.00 - 20.000	1.200
Forward Scattering Spectrometer Probe (FSSP)		
61 - 75	0.50 - 8.0	0.5
76 - 90	1.00 - 16.0	1.0
91 - 105	2.00 - 32.0	2.0
106 - 120	2.00 - 47.0	3.0

2.2.6 Particle Angular Scattering Measurements

The AFGL Abridged Polar Nephelometer (APN) measured angular scattering from particles at three wavelengths (0.66, 0.95 and 2.25 μm) and for three scattering angles (30, 100 and 140 degrees). The instrument subcomponents for each wavelengths were referred to as module 1, module 2 and module 3, respectively. The APN drew a sample of air into a cylindrical sampling volume and the scattered intensity at the three scattering angles was measured.

Table 4. A Sample of the Aerosol Data Reported at 1700 GMT, 6 October 1986

BIN NUMBER	MINIMUM DIAMETER (μm)	MAXIMUM DIAMETER (μm)	PARTICLE CONCENTRATION ($\# \ cm^{-3} \ \mu m^{-1}$)
1	0.320	0.349	6.368×10^{2}
2	0.349	0.378	2.122×10^{2}
3	0.378	0.407	2.122×10^{2}
4	0.407	0.436	1.061×10^{2}
5	0.436	0.465	1.061×10^{2}
6	0.465	0.494	5.306×10^{1}
7	0.494	0.523	5.306×10^{1}
9	0.552	0.581	1.592×10^{2}
11	0.610	0.639	5.306×10^{1}
15	0.726	0.755	5.306×10^{1}
16	0.500	0.650	3.077×10^{1}
18	0.800	0.950	1.025×10^{1}
31	1.000	1.750	0.4445
32	1.750	2.500	6.839×10^{-2}
33	2.500	3.250	0.1367
34	3.250	4.000	6.839×10^{-2}
39	7.000	7.750	3.419×10^{-2}
48	4.400	5.600	2.137×10^{-2}
49	5.600	6.800	2.137×10^{-2}
61	0.500	1.000	5.305×10^{-2}
64	2.000	2.500	5.305×10^{-2}
76	1.000	2.000	5.305×10^{-2}
91	2.000	4.000	3.315×10^{-3}
92	4.000	6.000	8.841×10^{-4}
94	8.000	10.000	2.210×10^{-4}
106	2.000	5.000	6.189×10^{-3}
107	5.000	8.000	4.420×10^{-4}

The APN data were provided every 15 minutes for limited time periods on 2, 4, 5 and 9 October 1986. The times of operation for the APN on 9 October 1986 are given in Figure 2. For the other days, the times of operation are given in Table 5.

Negative scattering intensities were occasionally reported for module 1 and module 2 and are clearly incorrect. These occurred during reported clear days and may represent system noise because the APN was not designed to be operated under very clear conditions. The data for module 3 are uncalibrated digital signal counts. In this form, these data cannot be used to obtain meaningful scattering information about the particles but can be used to look at variations in scattering.

Table 5. Time Periods of Operation, in LST, for the AFGL APN During the FTD Field Measurements Program

DATE	MODULE 1 (0.66μ m)	MODULE 2 (0.95 μm)	MODULE 3 (2.25 μm)
2 Oct 86	14:57-19:12	14:57-19:12	14:57-15:57 17:32-19:12
4 Oct 86	09:52-14:07 18:26-20:11	09:52-13:52 18:26-20:11	09:52-13:52 18:26-20:11
5 Oct 86	08:15-09:00	08:15-09:00	08:15-09:00

3. DISCUSSION OF DATA

3.1 Meteorological Data

The meteorological data: air temperature, dew point temperature, relative humidity, absolute humidity, wind speed and wind direction along with AWS surface weather observations are sufficient to reconstruct the weather events during the test period. Figures 3 (a.) to (d.) display the meteorological data obtained from the EMACS and Figures 4 to 8 show the (a.) surface and (b.) 500 mb maps[2] for the days of the tests. Tables 6 to 11 give the surface observations reported by the AWS observers.

The meteorological data taken by the EMACS have been compared against the routine surface observations taken by the AWS observers and the agreement between the data is good. The calibration points from the dew point temperature data have been removed and replaced with interpolated values.

3.2 Synoptic Conditions

3.2.1 6 October 1986

The data for 6 October demonstrate the effects of the passage of a cold front around 2200 LST on 5 October. The wind speeds peaked at the time of the frontal passage (see the note in the "Remarks" column in Table 6) and the wind direction shifted from west to north. The data for the rest

2. Climate Analysis Center (1986) Daily Weather Maps, Weekly Series 6-12 October 1986, National Oceanic and Atmospheric Administration, Washington, D. C.

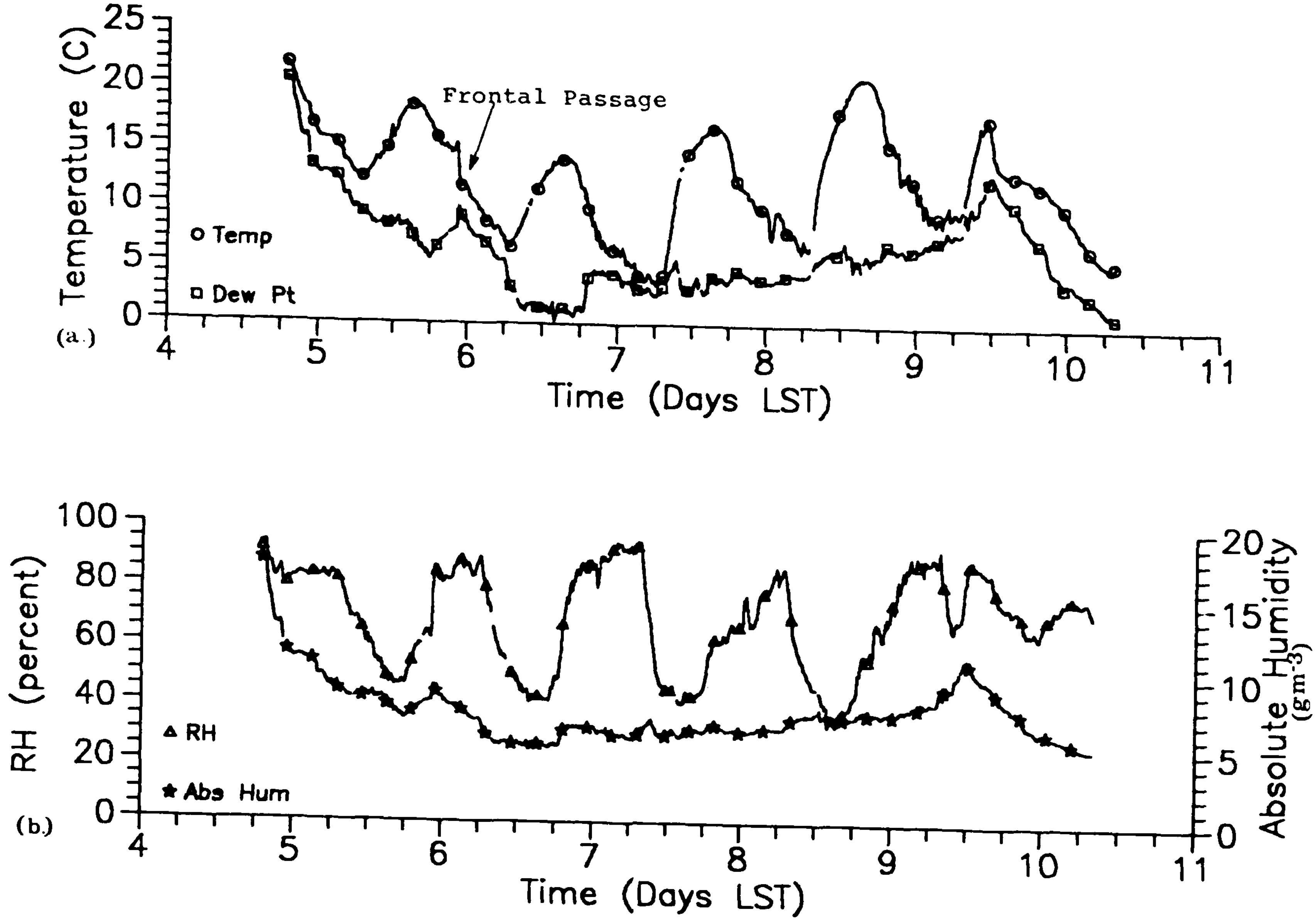

Figure 3. Meteorological Data for the Test Period 4-10 October 1986: (a.) Temperature and Dew Point Data and (b.) Relative and Absolute Humidity Data

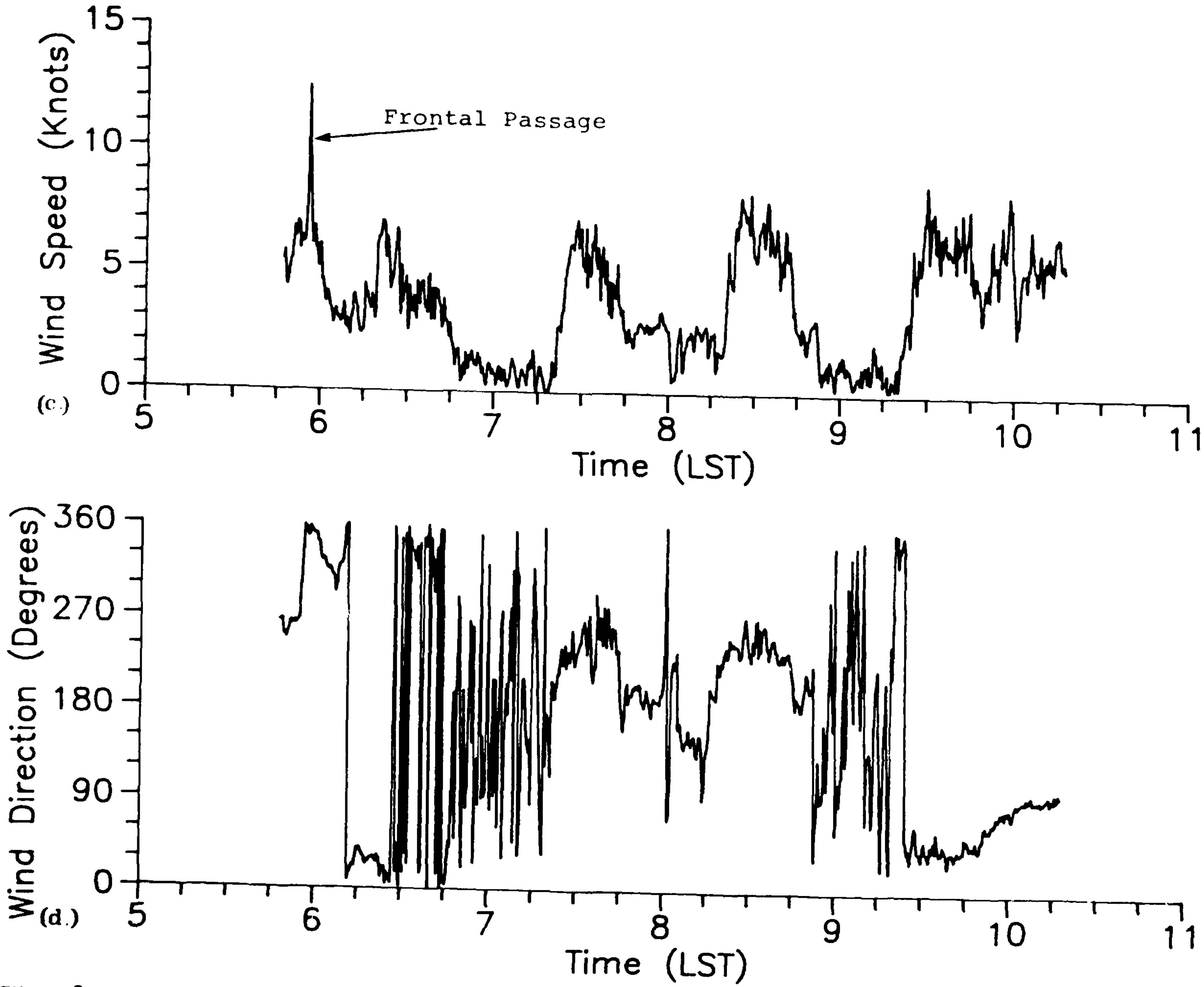

Figure 3. Meteorological Data for the Test Period 4-10 October 1986: (c.) Wind Speed and (d.) Wind Direction

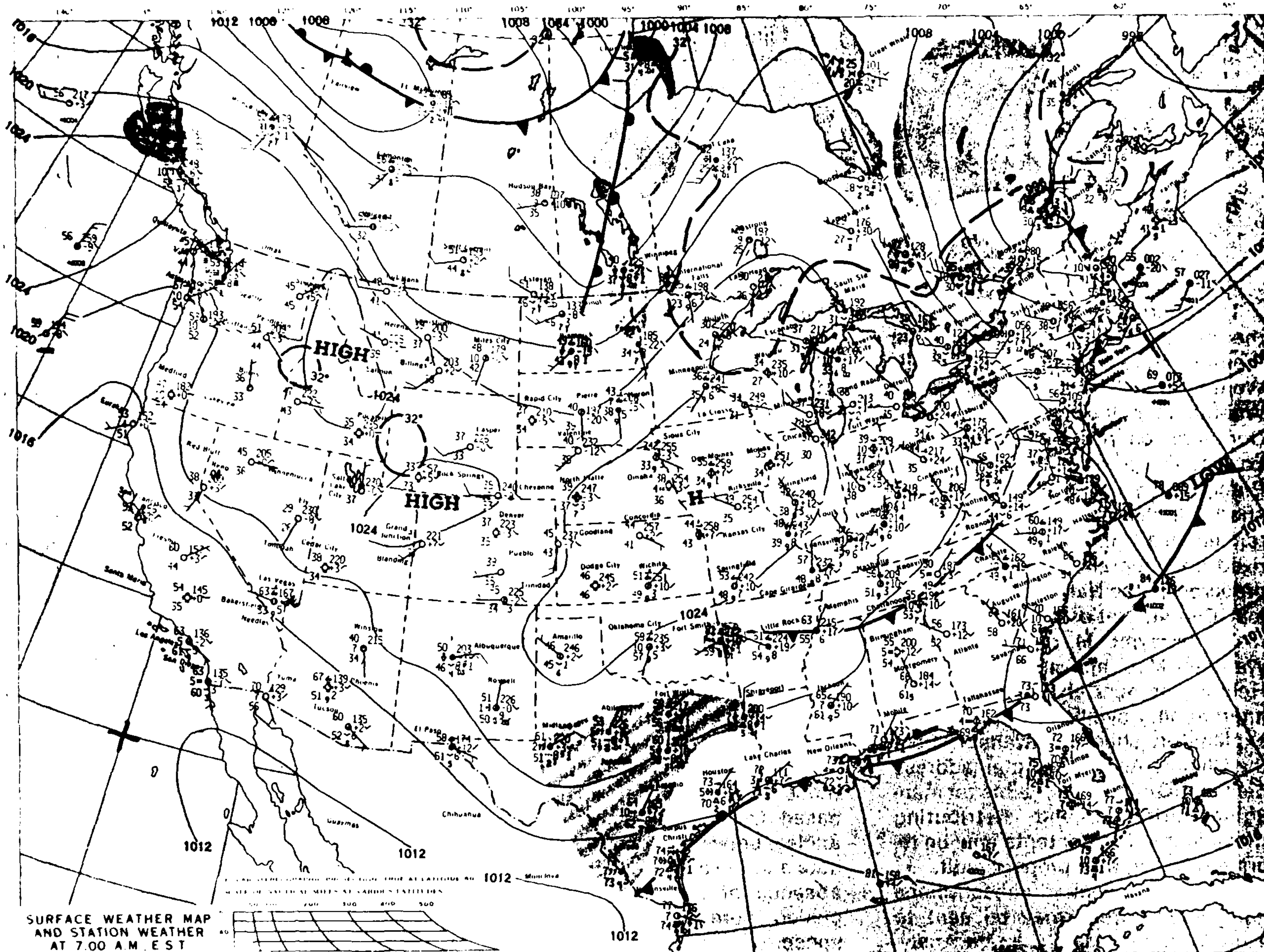

Figure 4. (a.) Surface Weather Map for 6 October 1986

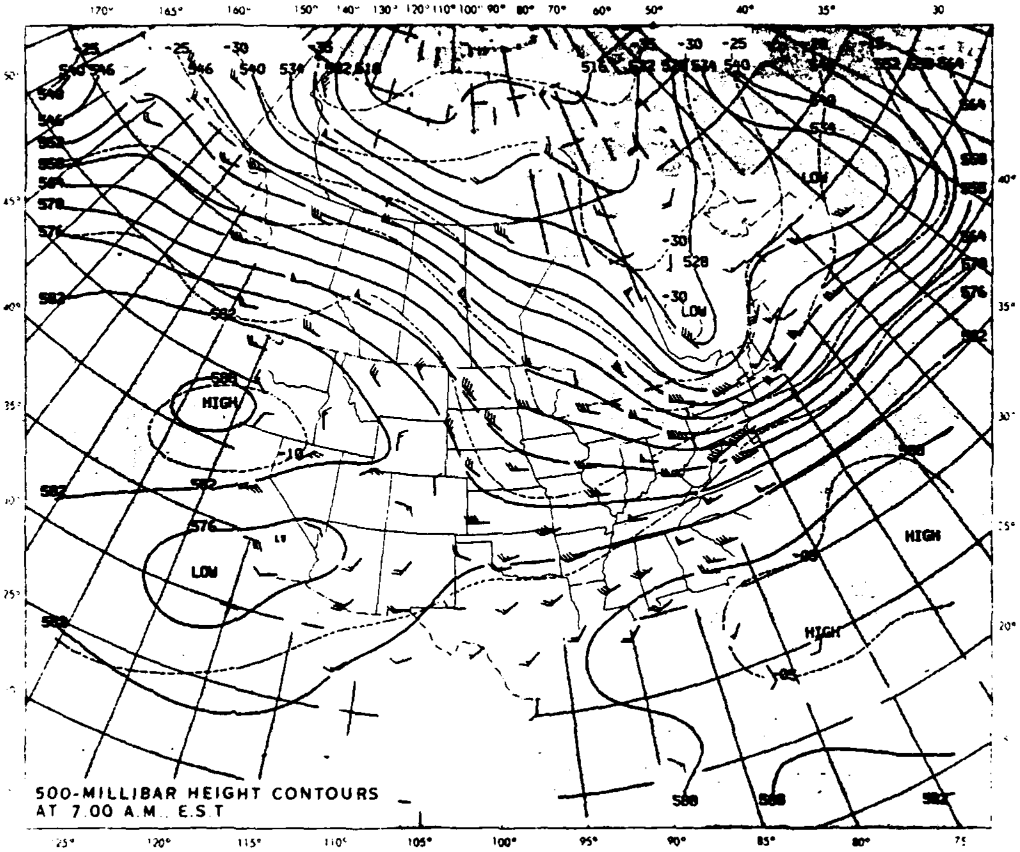

Figure 4. (b.) 500 mb Weather Map for 6 October 1986

Table 6. Air Weather Service Surface Observations for Wright-Patterson AFB, Ohio for 5 October 1986. (Subtract 5 Hours to Convert GMT to LST.)

TYPE	TIME (GMT)	SKY CONDITION	VISIBILITY (miles)	SEA LEVEL PRESS (mb)	TEMP (F)	DEW POINT (F)	WIND DIRECTION (deg)	WIND SPEED (knots)	REMARKS	STATION PRESSURE (in)	TOTAL SKY COVER
SA	0555	M28 BKN 120 OVC	15	119	62	55	31	08	11201 157/	29.020	10
SP	0616	E40 BKN 100 OVC	15				31	06			
SA	0655	15 SCT E40 BKN 100 OVC	15	122	62	54	29	07		29.030	10
SA	0755	E40 BKN	15	126	62	54	32	09		29.040	8
SA	0855	15 SCT E40 BKN	15	133	60	52	32	13	314 1500	29.060	9
SP	0947	M19 BKN 40 OVC	15				35	08			
SA	0955	M19 BKN 40 OVC	15	142	58	50	35	07		29.085	10
SA	1055	E20 BKN 40 OVC	15	146	57	49	34	08		29.095	10
SP	1143	20 SCT E40 BKN	15				36	06			
SA	1155	20 SCT E40 BKN	15	154	56	48	01	06	219 1500 20065	29.115	8
SA	1255	20 SCT 40 SCT 120 SCT	15	160	57	47	36	07	WND 30V02	29.130	4
SA	1355	20 SCT 40 SCT 120 SCT	15	162	58	47	02	08		29.135	4
SA	1456	E40 BKN 120 BKN	15	160	59	47	33	04	105 1570	29.130	8
SA	1555	E40 BKN	15	161	60	47	29	09		29.130	9
SA	1655	E40 BKN	15	156	62	47	25	04		29.115	6
SA	1756	40 SCT 200 SCT	15	149	64	46	26	06	812 1508	29.095	4
SA	1855	40 SCT 200 SCT	15	139	66	48	25	13	WND 21V28	29.070	4
SA	1955	40 SCT 200 SCT	15	134	67	46	27	10		29.055	4
SA	2055	40 SCT 200 SCT	15	134	68	46	27	12	WND 23V30 / 614 1508	29.055	4
SA	2155	120 SCT 200 SCT	20	133	67	44	28	12		29.050	5
SA	2255	70 SCT 120-BKN 200-BKN	20	136	64	43	27	10	WND 23V30	29.060	7
SA	2355	70 SCT 200 SCT	20	139	61	44	26	06	303 1078	29.065	3
SA	0055	70 SCT 200 SCT	20	141	60	45	25	08		29.070	3
SA	0155	40 SCT	20	147	60	45	25	08		29.090	5
SA	0255	E40 BKN	20	151	59	46	27	09	212 1500	29.100	8
SP	0315	E40 OVC	20				33	18	WND 27V36 WSHFT IS PROPA		
SP	0335								WR//		
SA	0355	20 SCT E40 OVC	15	174	54	47	33	09	WND 30V36 PRESRR WR//	29.160	10
SP	0406	E40 BKN	20				33	10			
SA	0455	E40 BKN	20	176	55	47	33	11	WR//	29.170	7

Table 7. Air Weather Service Surface Observations for Wright-Patterson AFB, Ohio for 6 October 1986. (Subtract 5 Hours to Convert GMT to LST.)

TYPE	TIME (GMT)	SKY CONDITION	VISIBILITY (miles)	SEA LEVEL PRESS (mb)	TEMP (F)	DEW POINT (F)	WIND DIRECTION (deg)	WIND SPEED (knots)	REMARKS	STATION PRESSURE (in)	TOTAL SKY COVER
SA	0555	CLR	20	180	53	45	31	02	12701 WR//	29.180	0
SA	0655	CLR	20	186	52	44	00	00	WR//	29.200	0
SA	0755	CLR	20	189	50	43	00	00		29.210	0
SA	0355	CLR	20	195	50	42	31	02	215	29.225	0
SA	0955	20 SCT 250 SCT	20	201	50	42	36	05		29.240	3
SA	1055	20 SCT 250 SCT	20	210	49	39	36	06		29.270	5
SA	1155	20 SCT 250 SCT	20	216	47	36	02	05	220 1501 20001	29.285	5
SA	1256	40 SCT 150 SCT 200 SCT	20	228	48	36	36	02		29.310	5
SA	1355	40 SCT 100 SCT 150 SCT	20	228	50	34	35	08	WND 31V03	29.310	4
SA	1457	100 SCT 150 SCT	20	236	53	34	36	04	119 1080	29.340	3
SA	1558	40 SCT 100 SCT 150 SCT	20	238	54	34	31	07		29.345	2
SA	1656	40 SCT 150 SCT	20	231	55	35	36	04		29.325	2
SA	1758	40 SCT 150 SCT	20	226	57	33	E33	12	710 1570	29.310	1
SA	1857	50 SCT 150 SCT	20	217	58	34	E04	05		29.285	2
SA	1955	50 SCT 150 SCT	20	214	58	33	E34	05		29.275	2
SA	2055	50 SCT 150 SCT 200 SCT	20	211	58	35	E01	05	614 1571	29.270	1
SA	2155	50 SCT	20	209	57	34	33	04		29.260	1
SA	2255	50 SCT	20	210	55	34	36	03		29.260	1
SA	2355	50 SCT	20	214	54	36	00	00	302 1500	29.275	1
SA	0055	50 SCT	20	216	51	38	00	00		29.280	1
SA	0155	50 SCT	20	221	48	39	00	00		29.290	1
SA	0255	CLR	20	222	46	37	00	00	208	29.300	0
SA	0355	50 SCT	20	222	46	38	00	00		29.300	3
SA	0455	250 SCT	20	223	47	39	00	00		29.300	3

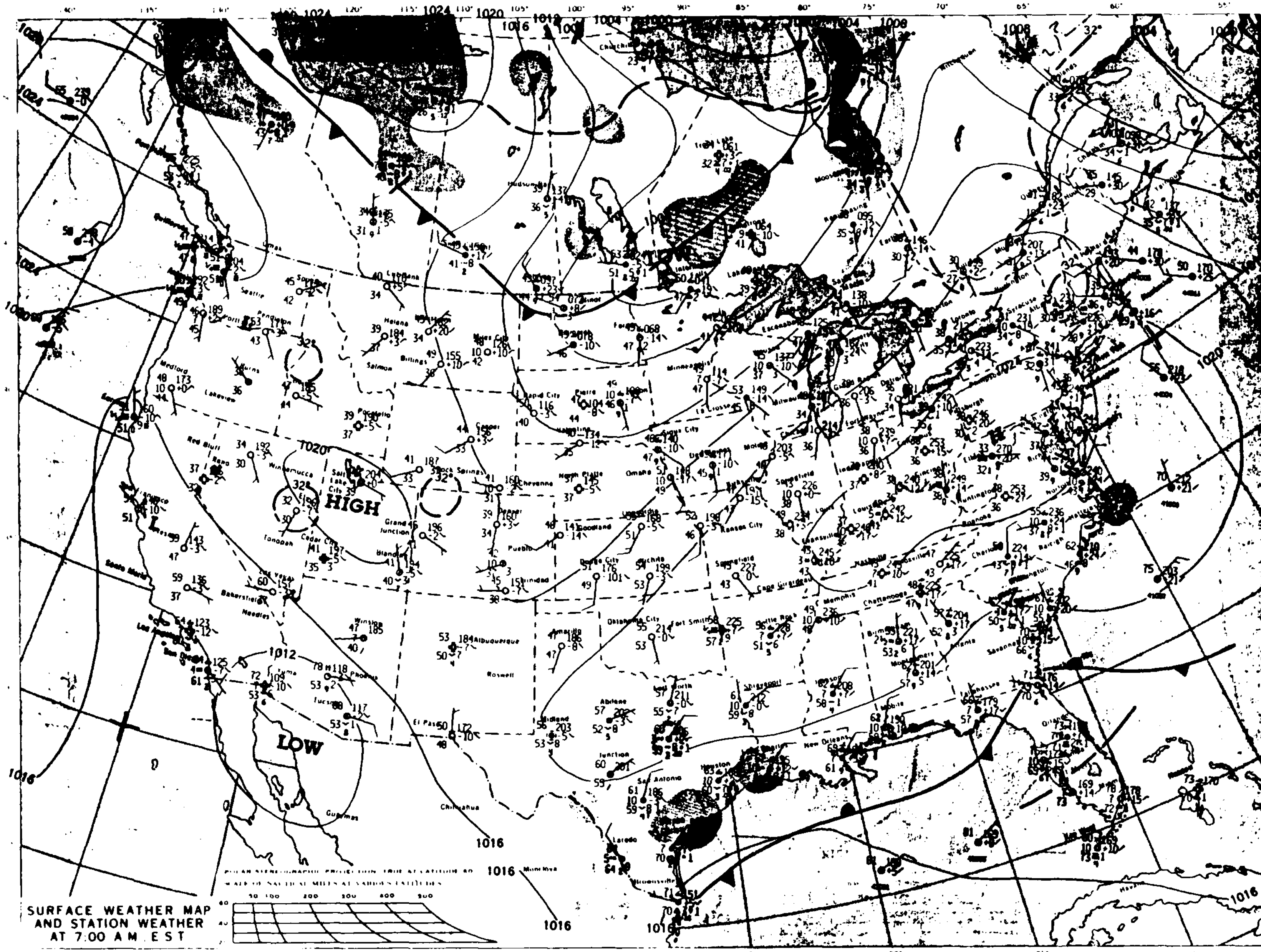

Figure 5. (a.) Surface Weather Map for 7 October 1986

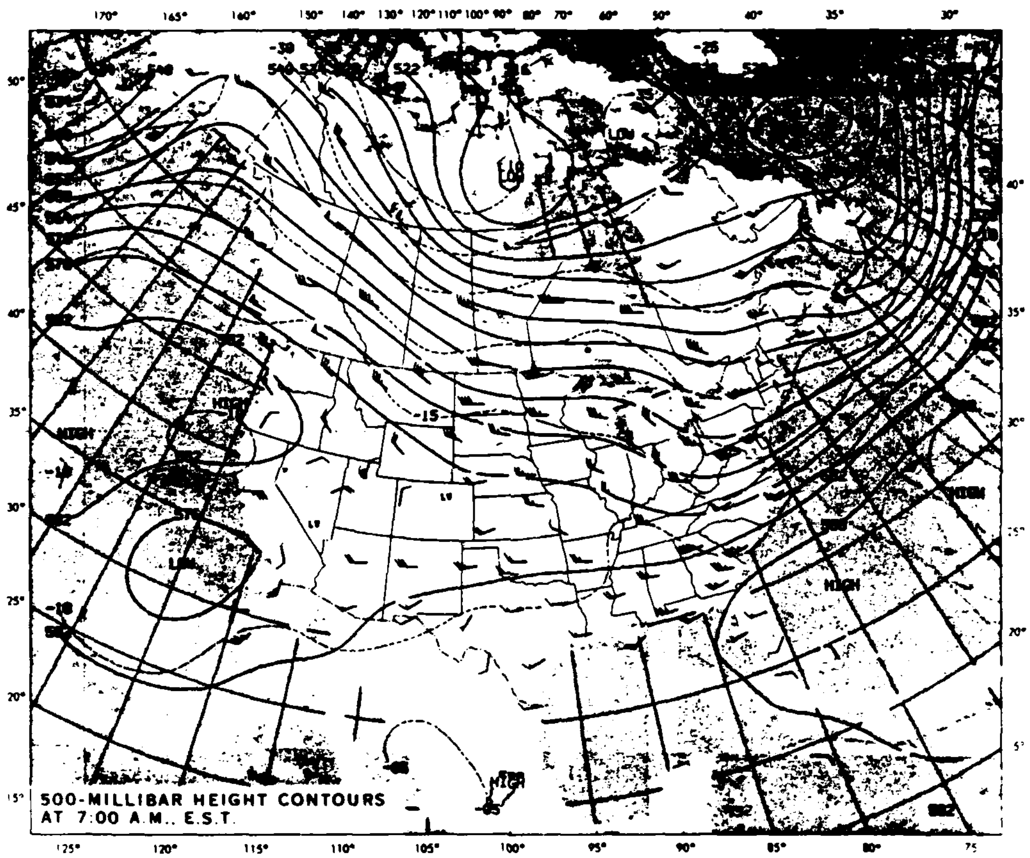

Figure 5. (b.) 500 mb Weather Map for 7 October 1986

Table 8. Air Weather Service Surface Observations for Wright-Patterson AFB, Ohio for 7 October 1986. (Subtract 5 Hours to Convert GMT to LST.)

TYPE	TIME (GMT)	SKY CONDITION	VISIBILITY (miles)	SEA LEVEL PRESS (mb)	TEMP (F)	DEW POINT (F)	WIND DIRECTION (deg)	WIND SPEED (knots)	REMARKS	STATION PRESSURE (in)	TOTAL SKY COVER
SA	0555	250 SCT	20	220	46	39	00	00	803 1001	29.290	2
SA	0655	CLR	20	227	42	37	00	00		29.310	0
SA	0755	CLR	20	226	43	37	00	00		29.310	0
SA	0855	CLR	20	226	43	37	00	00	107	29.310	0
SA	0955	250-SCT	20	235	43	35	00	00		29.330	1
SA	1055	CLR	20	238	42	35	00	00		29.340	0
SA	1155	CLR	20	241	42	35	00	00	SHLW GP SW/ 214	29.350	0
SA	1255	CLR	9	242	46	37	00	00		29.350	0
SA	1357	CLR	9	244	52	39	00	00		29.360	0
SA	1455	CLR	9	244	57	42	19	03	103	29.360	0
SA	1555	CLR	10	240	60	39	21	08		29.350	0
SA	1655	250 SCT	10	237	61	38	23	06		29.340	1
SA	1756	250-SCT	13	229	63	40	22	05	814 1001	29.320	1
SA	1856	250-SCT	12	220	64	40	23	07	WND 19V27	29.290	1
SA	1955	250-SCT	12	214	64	39	23	06		29.275	1
SA	2055	CLR	10	211	64	40	22	04	719	29.265	0
SA	2155	CLR	10	208	64	40	21	03		29.255	0
SA	2256	CLR	15	207	61	40	20	03		29.250	0
SA	2355	CLR	15	201	58	39	19	03	610	29.235	0
SA	0055	CLR	20	206	57	39	20	04		29.250	0
SA	0155	CLR	20	205	53	39	00	00		29.250	0
SA	0255	CLR	20	201	54	39	00	00	602	29.240	0
SA	0355	CLR	20	200	50	39	00	00		29.235	0
SA	0455	CLR	20	199	50	39	00	00		29.235	0

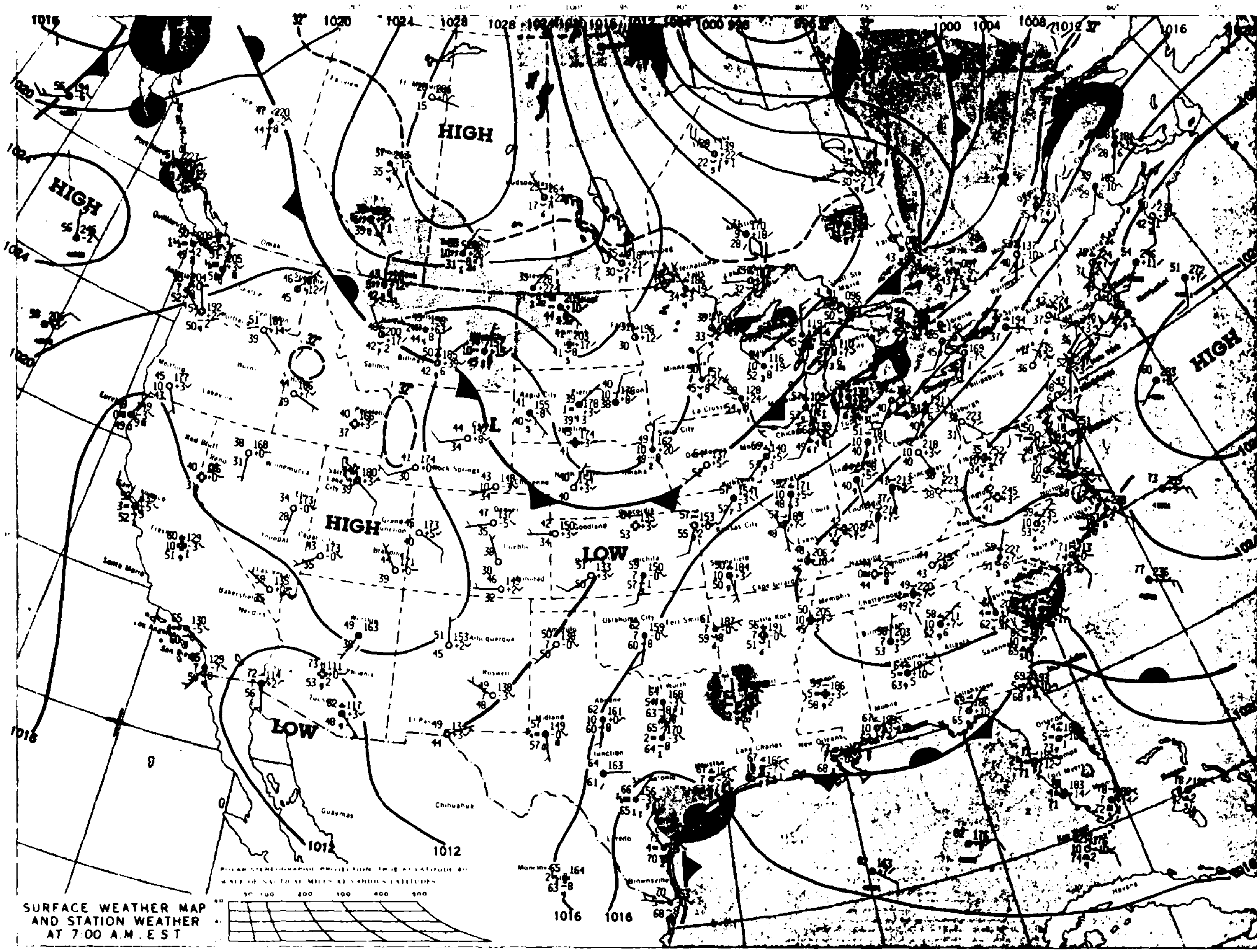

Figure 6. (a.) Surface Weather Map for 8 October 1986

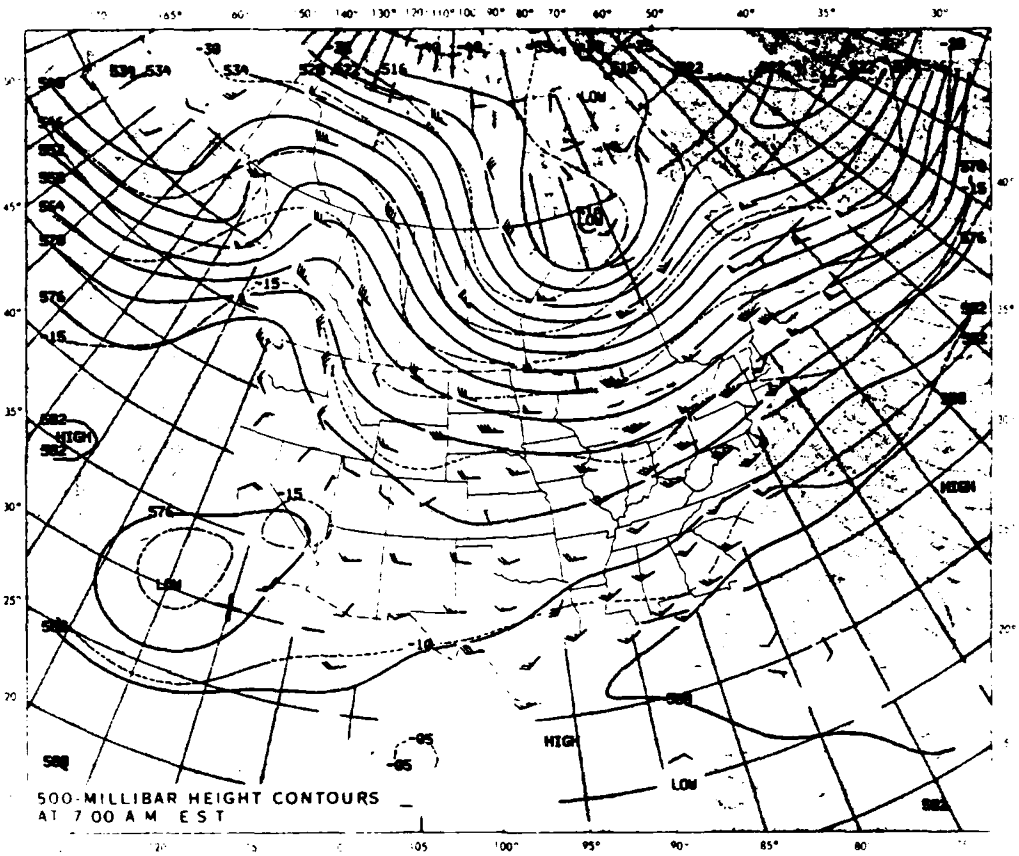

Figure 6. (b.) 500 mb Weather Map for 8 October 1986

Table 9. Air Weather Service Surface Observations for Wright-Patterson AFB, Ohio for 8 October 1986. (Subtract 5 Hours to Convert GMT to LST.)

TYPE	TIME (GMT)	SKY CONDITION	VISIBILITY (miles)	SEA LEVEL PRESS (mb)	TEMP (F)	DEW POINT (F)	WIND DIRECTION (deg)	WIND SPEED (knots)	REMARKS	STATION PRESSURE (in)	TOTAL SKY COVER
SA	0555	CLR	20	199	49	39	00	00	602	29.235	0
SA	0655	CLR	20	201	50	40	00	00		29.240	0
SA	0755	CLR	20	199	48	38	00	00		29.235	0
SA	0855	CLR	20	199	47	39	00	00	000	29.235	0
SA	0955	CLR	20	199	47	38	00	00		29.235	0
SA	1055	CLR	20	205	47	39	00	00		29.250	0
SA	1155	80 SCT	10	205	47	38	00	00	105 1070	29.250	2
SA	1255	80 SCT	10	207	51	41	17	01		29.255	1
SA	1355	80 SCT	10	207	58	43	22	06		29.255	1
SA	1457	80 SCT	10	202	46		21	08	802 1070 46 COR14	29.245	1
SA	1555	80 SCT	10	M	61	45	E23	10		E29.235	1
SA	1657	100 SCT	13	193	69	45	22	08	ALSTG 011 COR13	29.220	1
SA	1755	100 SCT	13	190	71	47	24	06	708 1070	29.210	1
SA	1855	250 SCT	13	183	72	46	E25	10		29.190	1
SA	1955	250 SCT	13	178	72	46	E21	09		29.180	1
SA	2055	250 SCT	10	177	72	46	E18	08	612 1001	29.175	1
SA	2156	150 SCT 250 SCT	10	183	72	46	E18	10		29.190	2
SA	2255	150 SCT 250 SCT	15	183	72	46	E21	04		29.190	2
SA	2358	150 SCT 250 SCT	15	188	66	47	E20	03	310 1071	29.205	2
SA	0055	150 SCT	20	192	64	41	E22	02		29.215	1
SA	0156	150 SCT	20	195	59	46	E00	00		29.220	2
SA	0255	CLR	20	194	60	46	00	00	105	29.220	0
SA	0355	CLR	20	196	57	46	00	00		29.225	0
SA	0455	CLR	20	190	56	46	00	00		29.215	0

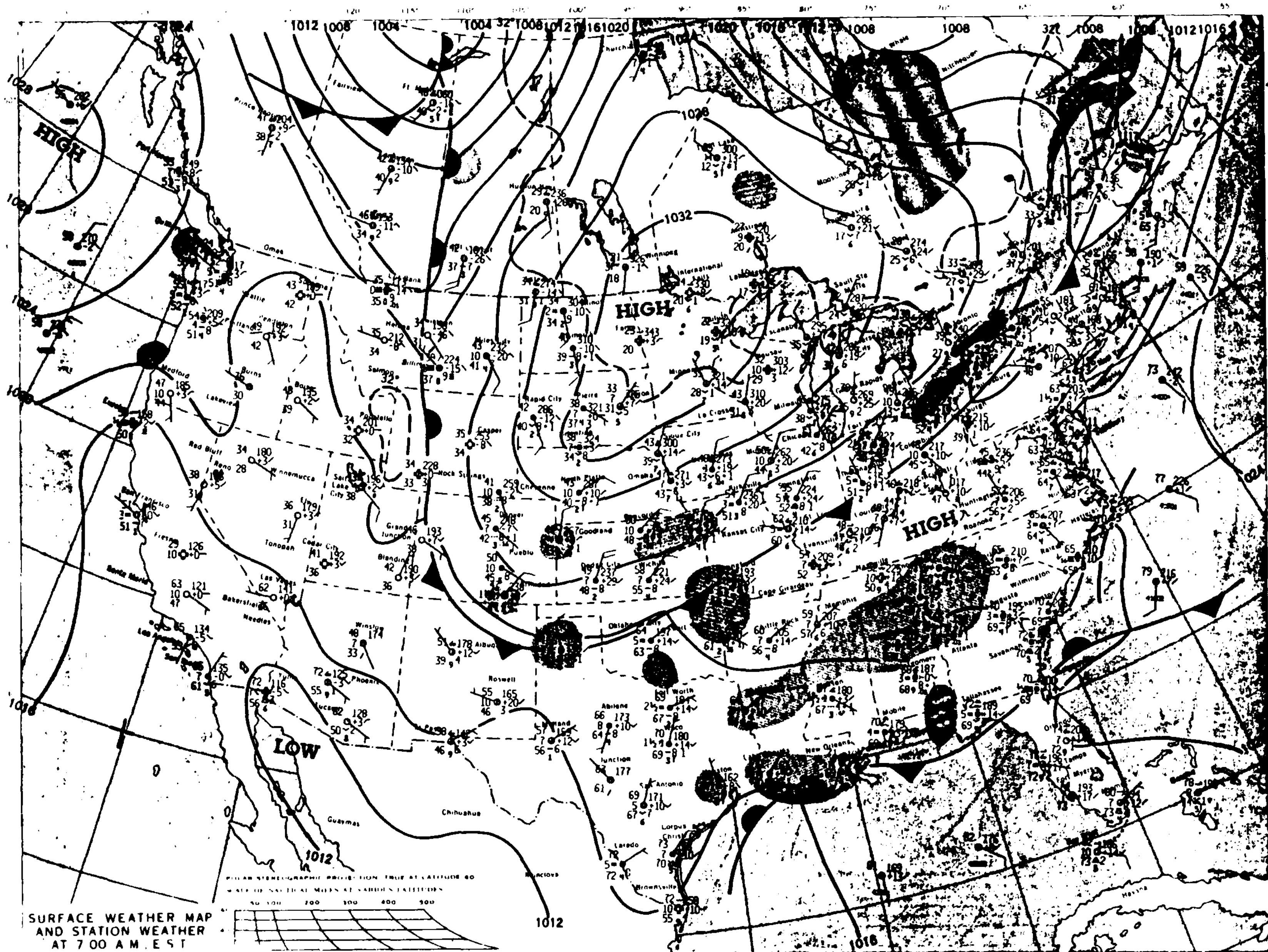

Figure 7. (a.) Surface Weather Map for 9 October 1986

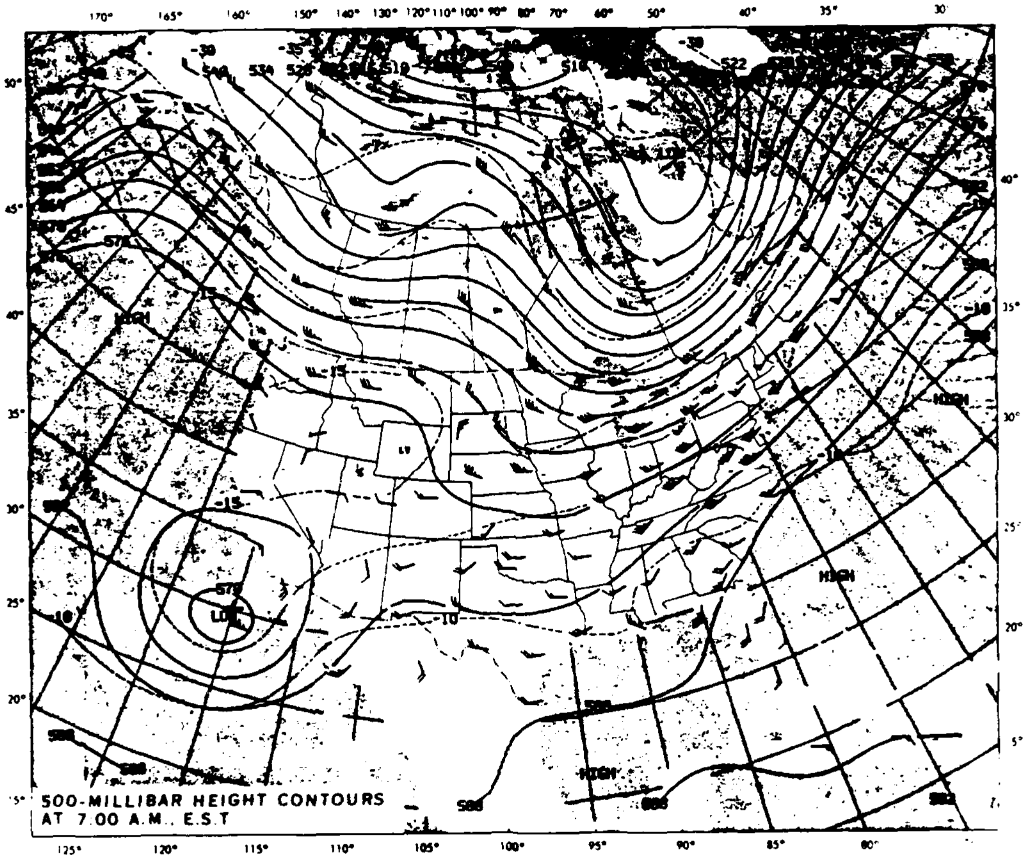

Figure 7. (b.) 500 mb Weather Map for 9 October 1986

Table 10. Air Weather Service Surface Observations for Wright-Patterson AFB, Ohio for 9 October 1986. (Subtract 5 Hours to Convert GMT to LST.)

TYPE	TIME (GMT)	SKY CONDITION	VISIBILITY (miles)	SEA LEVEL PRESS (mb)	TEMP (F)	DEW POINT (F)	WIND DIRECTION (deg)	WIND SPEED (knots)	REMARKS	STATION PRESSURE (in)	TOTAL SKY COVER
SA	0555	CLR	20	192	55	46	00	00	500	29.220	0
SA	0655	CLR	15	195	54	47	00	00		29.230	0
SA	0755	CLR	15	196	51	46	00	00		29.230	0
SA	0855	E70 BKN	10	196	51	46	00	00	103 1070	29.230	7
SA	0955	20 SCT E70 BKN	10	204	54	48	14	01		29.250	7
SA	1055	20 SCT E70 OVC	10	208	53	47	00	00		29.260	10
SA	1155	30 SCT 70 SCT	5 Fog	209	53	48	00	00	112 1570	29.265	4
SA	1255	30 SCT 70 SCT	5 Fog	214	55	51	00	00		29.280	3
SA	1355	30 SCT 200 SCT	6 Fog	216	59	52	00	00		29.285	1
SA	1455	30 SCT E80 BKN	8	220	62	59	02	04	212 1570	29.300	9
RS	1555	M28 BKN 80 BKN	9	222	64	60	02	06		29.305	8
SA	1655	E18 BKN 28 OVC	7	229	61	59	02	10		29.325	10
SP	1735	M10 BKN 20 OVC	7				02	08		29.330	10
SA	1755	M11 BKN 20 OVC	9	232	59	56	02	07	210 15//	29.330	10
SA	1855	M11 BKN 20 OVC	7	232	58	56	04	08		29.330	10
SA	1955	M14 BKN 20 OVC	9	235	58	53	04	08		29.340	10
SA	2055	M14 OVC	10	240	57	51	02	08	307 15//	29.350	10
SP	2148	14 SCT M22 OVC	10				04	08			
SA	2157	14 SCT M22 OVC	10	240	59	49	04	08		29.350	10
SA	2255	M28 OVC	10	243	57	48	03	10		29.360	10
SA	2357	M28 OVC	13	245	56	47	04	06	307 15//	29.370	10
SA	0055	M28 OVC	13	248	57	47	03	04		24.380	10
SP	0121	28 SCT M38 OVC	13				04	08			
SA	0155	M38 OVC	13	252	55	44	04	08		29.390	10
SA	0259	E45 OVC	13	258	55	42	05	10	210 15//	29.405	10
SA	0355	E50 OVC	15	254	52	41	05	08		29.395	10
SA	0456	E50 BKN	20	257	52	41	07	10		29.400	8

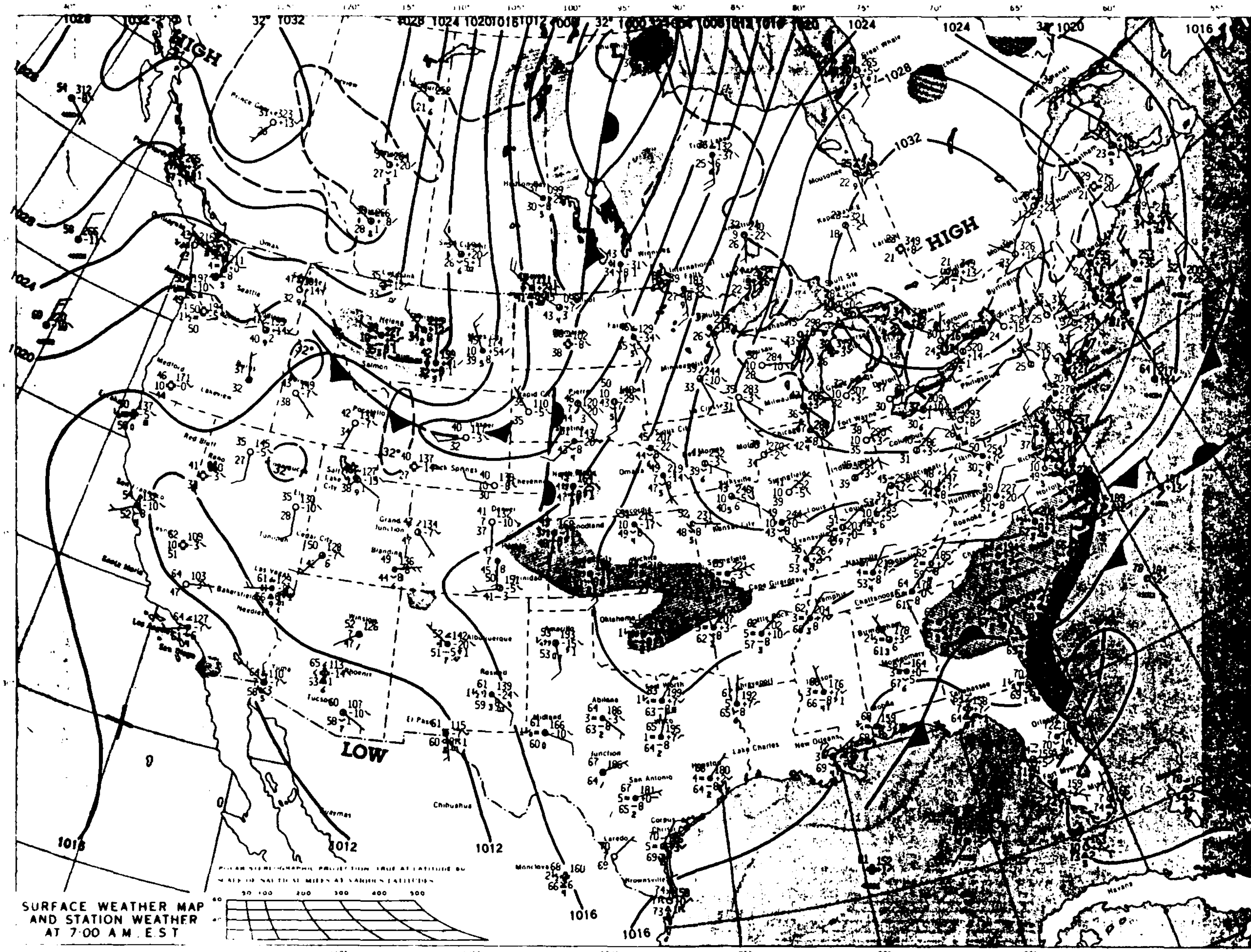

Figure 8. (a.) Surface Weather Map for 10 October 1986

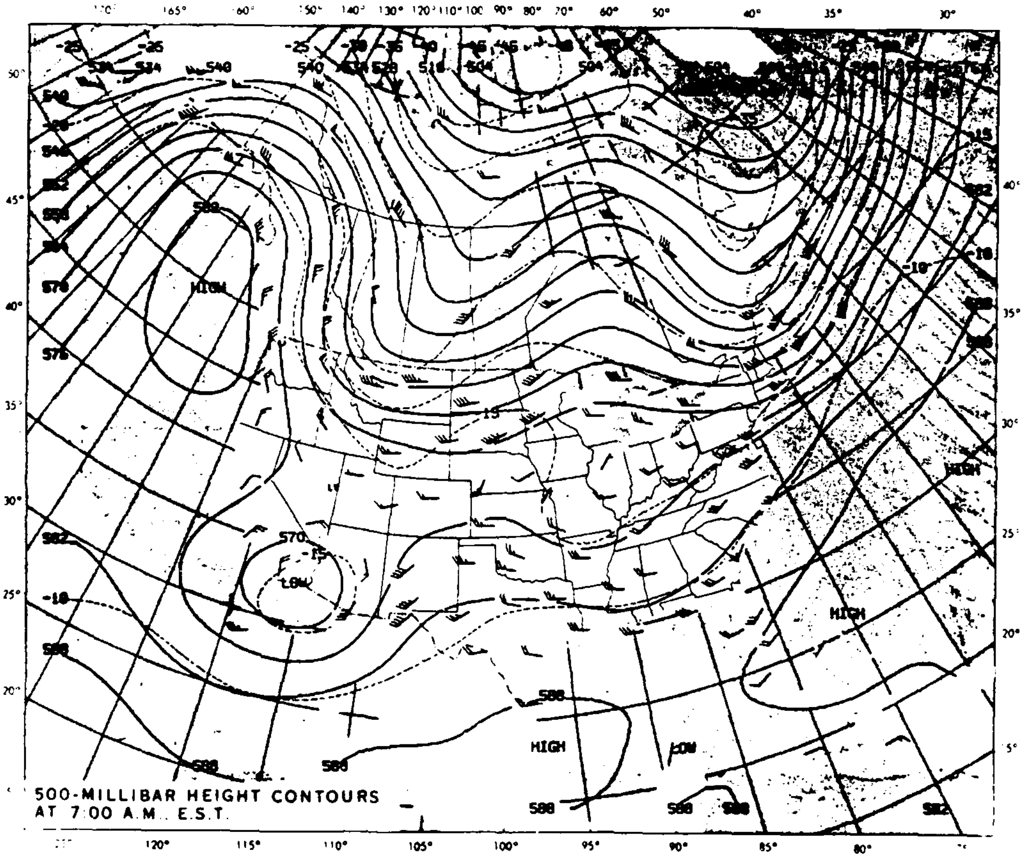

Figure 8. (b.) 500 mb Weather Map for 10 October 1986

Table 11. Air Weather Service Surface Observations for Wright-Patterson AFB, Ohio for 10 October 1986. (Subtract 5 Hours to Convert GMT to LST.)

TYPE	TIME (GMT)	SKY CONDITION	VISIBILITY (miles)	SEA LEVEL PRESS (mb)	TEMP (F)	DEW POINT (F)	WIND DIRECTION (deg)	WIND SPEED (knots)	REMARKS	STATION PRESSURE (in)	TOTAL SKY COVER
SA	0555	50 SCT	20	260	50	40	06	06	302 1500	29.410	4
SA	0655	50 SCT 90 SCT	20	264	49	39	06	06		29.420	3
SA	0756	90 SCT	20	265	48	38	06	07		29.420	2
SA	0855	90 SCT	20	265	47	38	07	06	103 1070	29.420	2
SA	0955	CLR	20	267	46	37	07	06		29.425	0
SA	1055	CLR	20	269	45	36	06	08		29.430	0
SA	1156	150 SCT	20	271	45	35	07	07	305 1070	29.435	2
SA	1256	200 SCT	20	273	47	35	08	07		29.445	1
SA	1355	200 SCT	20	271	49	35	08	10		29.440	1
SA	1455	200 SCT	15	269	53	36	06	08	802 1008	29.430	1
SA	1555	200 SCT	15	262	55	35	09	08		29.415	1
SA	1657	200 SCT	15	257	58	35	07	07		29.400	2
SA	1755	200 SCT	15	247	61	36	08	08	WND 03V13 / 820 1001	29.370	2
SA	1855	200 SCT	15	240	63	36	07	08		29.350	4
SA	1955	200 SCT	15	236	64	36	05	06		29.340	2
SA	2057	250 SCT	15	229	64	37	04	06	717 1002	29.320	2
SA	2155	250 SCT	15	229	63	37	05	05		29.320	2
SA	2255	200 SCT 250 SCT	15	232	59	38	05	04		29.325	3
SA	2355	250 SCT	15	233	53	39	05	04	102 1002	29.325	3
SA	0055	250 SCT	15	231	53	39	05	04		29.320	2
SA	0155	250 SCT	15	232	53	37	05	03		29.320	2
SA	0255	250 SCT	15	228	52	37	08	03	703 1001	29.315	1
SA	0355	250 SCT	15	226	52	37	07	03		29.310	1
SA	0455	250 SCT	15	225	52	38	06	01		29.310	1

of the day indicate a clear day with diurnal variations of temperature and humidity.

3.2.2 7 & 8 October 1986

The data for 7 October show a day that was clear and dry, a large diurnal range in temperature, little moisture change and a boundary layer break-up after sunrise (0700 LST) as signified by the increase in the wind speeds. The data for 8 October show similar trends.

3.2.3 9 October 1986

A weak front (e.g. Figure 7) moved through the area during the day as noted by the drop off in temperatures around 1100 LST. The frontal passage did not produce any precipitation as verified by the AWS observations taken about 7.5 km away. Fog was reported around sunrise, with visibilities reported to be 5 miles. The fog was not dense, however, and may reflect the fact that observers are required to report visibilities of 5 miles or less as fog.

As the front went through, skies became cloudy and the air and dew point temperatures started to drop. Due to the light winds preceding the frontal passage, there was not much of a sign in the wind data that a front had gone through. The wind directions began to blow out of the north northeast after the frontal passage. There was a sharp increase in the dew point temperatures of 9° F four hours preceding the front. This was responsible in part for the high relative humidities observed around sunrise.

3.2.4 10 October 1986

High pressure centered over southwest Quebec (e.g. Figure 8 (a.)) was building south, bringing somewhat cooler and much drier air to the Dayton area. A strong indication of the new Canadian air mass was the drop in dew point from the lower 60's to the mid 30's by midday on the 10 October. Because of the moderate winds overnight, temperatures did not cool off significantly.

3.3 Transmission Data

The transmission data at four selected wavelengths, 0.497, 0.551, 1.059 and 10.51 μm are displayed as a function of time in Figure 9. For comparison purposes, Figure 10 (a.) displays the data for the two visible wavelengths and Figure 10 (b.) displays the data for the two infrared wavelengths. In examining the figures, one should remember that the wavelengths displayed are only a subset of the complete transmission data set and that not all of the wavelengths were availiable all of the time. Thus, comparisons between the visible and the IR transmission data were not always possible.

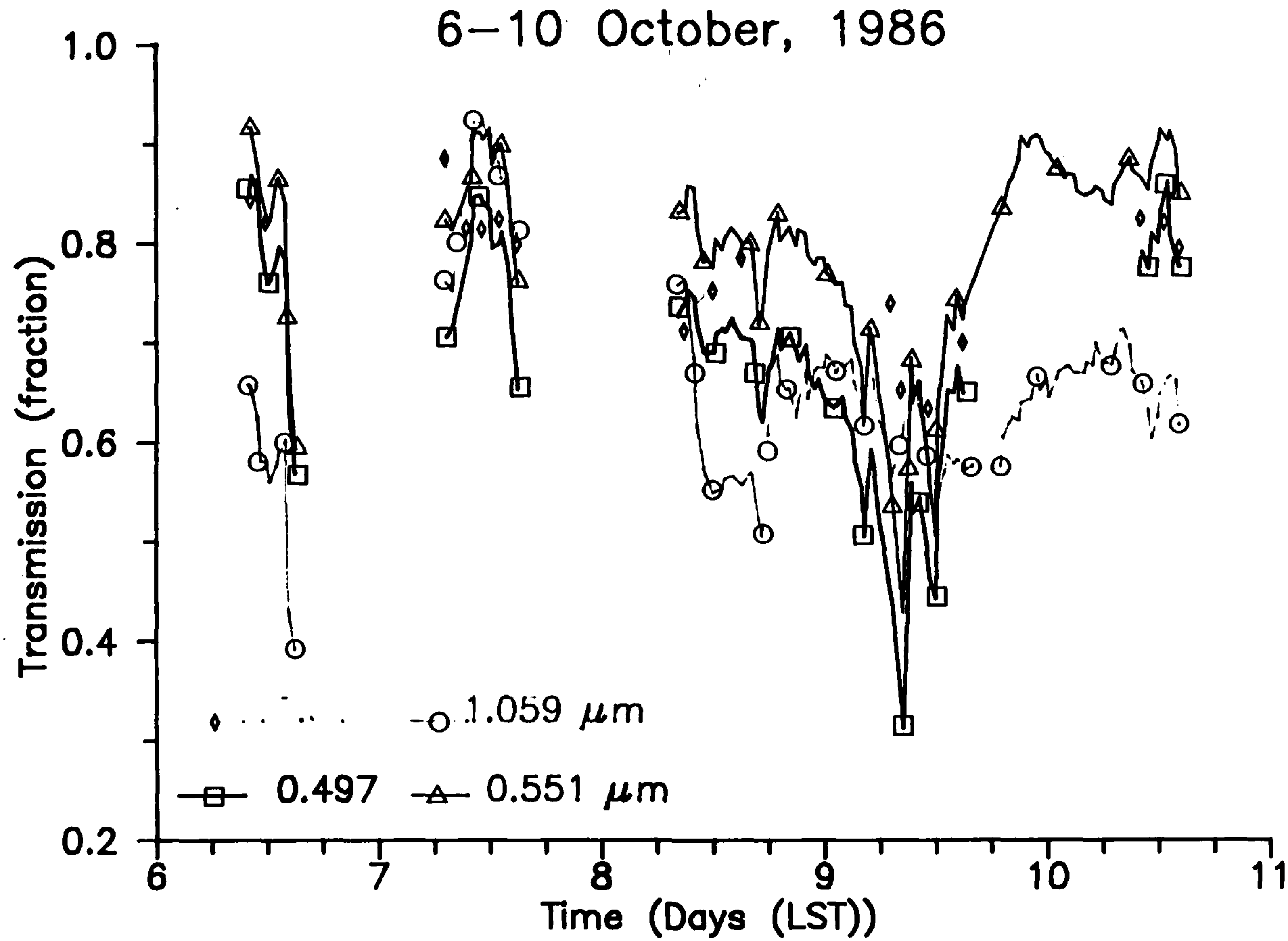

Figure 9. Selected Transmission Data as a Function of Time for the Period 6-10 October 1986

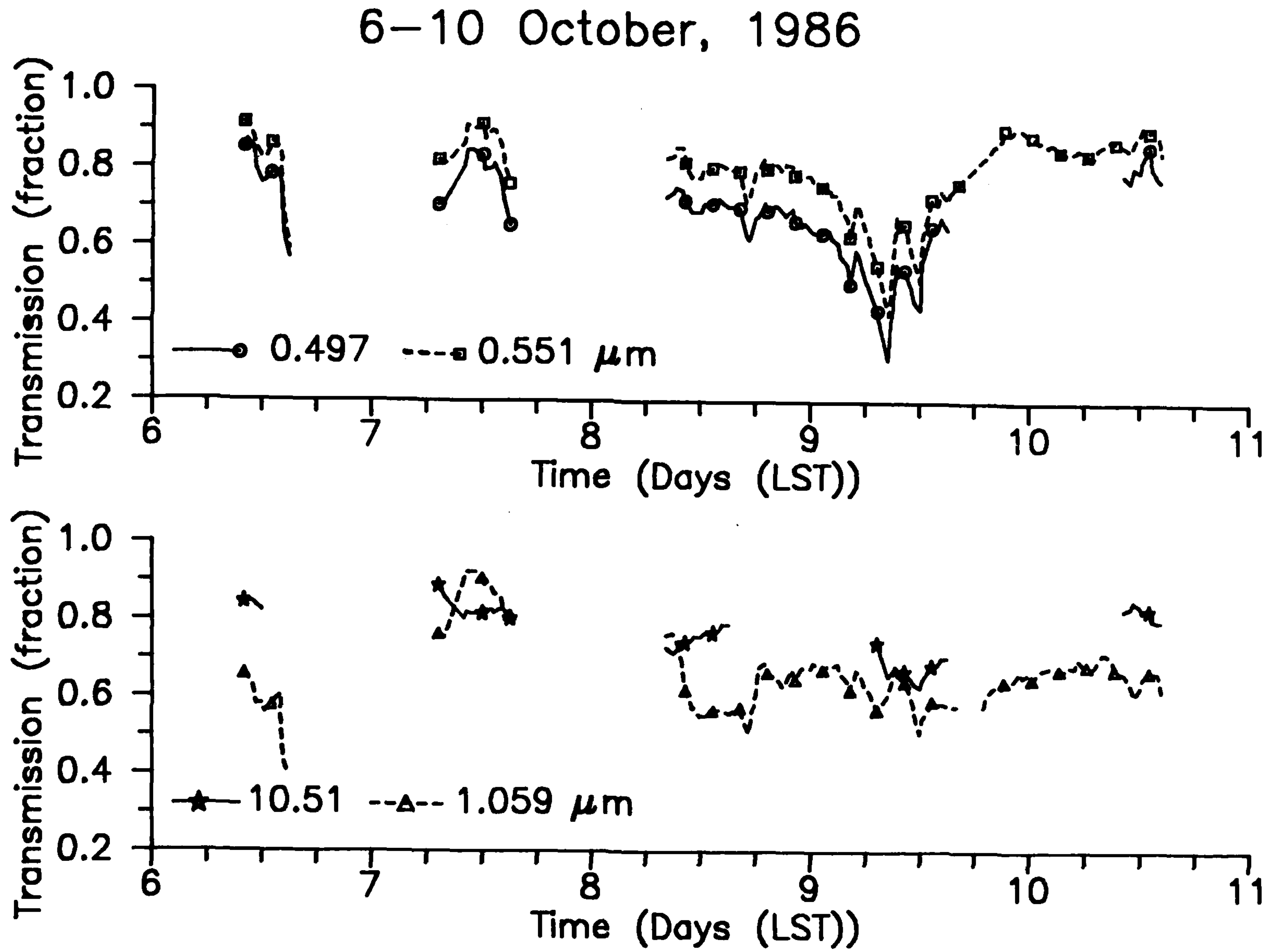

Figure 10. Transmission Data as a Function of Time for (a.) the Two Selected Visible Wavelengths and (b.) the Two Selected Infrared Wavelengths for the Period 6-10 October 1986

3.3.1 Visible Transmission

The visible transmission data, to a large extent, qualitatively agree with the environmental data. The visible transmission data change with respect to absolute humidity as one would expect. That is, as absolute humidity increases, transmission decreases. Also, the visible transmission data qualitatively agree with the visual quality data (see Section 3.4.1) in that as the transmission decreased, the visual quality data increased. There are notable exceptions to the qualitative agreement, however.

On 6 October between 1000-1500 LST, the visible (and near IR) transmissions drop dramatically, yet the absolute humidity changes very little. The AWS-reported visibilities and visual quality data show generally stable values and values reflective of a clear atmosphere. The cause of this discrepency is not known.

3.3.2 IR Transmission

The IR transmission data appear to suffer from some major inconsistencies. The 1.059 μm data from 6 October track the visible wavelength data reasonably well but exhibit magnitudes that are significantly below the visible data. One would expect the 1.059 μm transmissions to be nearly equal to or somewhat larger than the 0.551 μm values, assuming the presence of typical background aerosols and gases.

The data for 7 October are also suspect. The 1.059 μm data again track the visible data as expected but the magnitudes relative to the visible values are changing. That is, sometimes the 1.059 μm data are greater than the visible values and at other times the visible data values are larger. The 10.51 μm transmission data track opposite to the visible data. That is, as the visible data increase, the 10.51 μm values decrease. This is shown more clearly in Figure 11 in which only the 0.551 and 10.51 μm data are displayed. We have no explanations for these inconsistencies.

3.4 Visual Quality and Visual Range Data

The visual quality and visual range data are displayed in Figure 12. For comparison purposes the transmission values at 0.551 μm are also displayed.

3.4.1 Visual Quality

The visual quality data from the integrating nephelometer qualitatively agree with the prevailing visibilities reported by the AWS observers. Generally clear conditions were reported on 6 October following the frontal passage and this is seen in the nephelometer data. The decreases in visibility reported on 8 October between 0600-1100 LST can also be seen in the data, as well as the decreases seen on 9 October that are associated with the presence of fog.

A weak diurnal cycle can be seen in the data that agrees with the diurnal variation in relative humidity (e.g. Figure 3(b.)). The visual quality data generally achieved

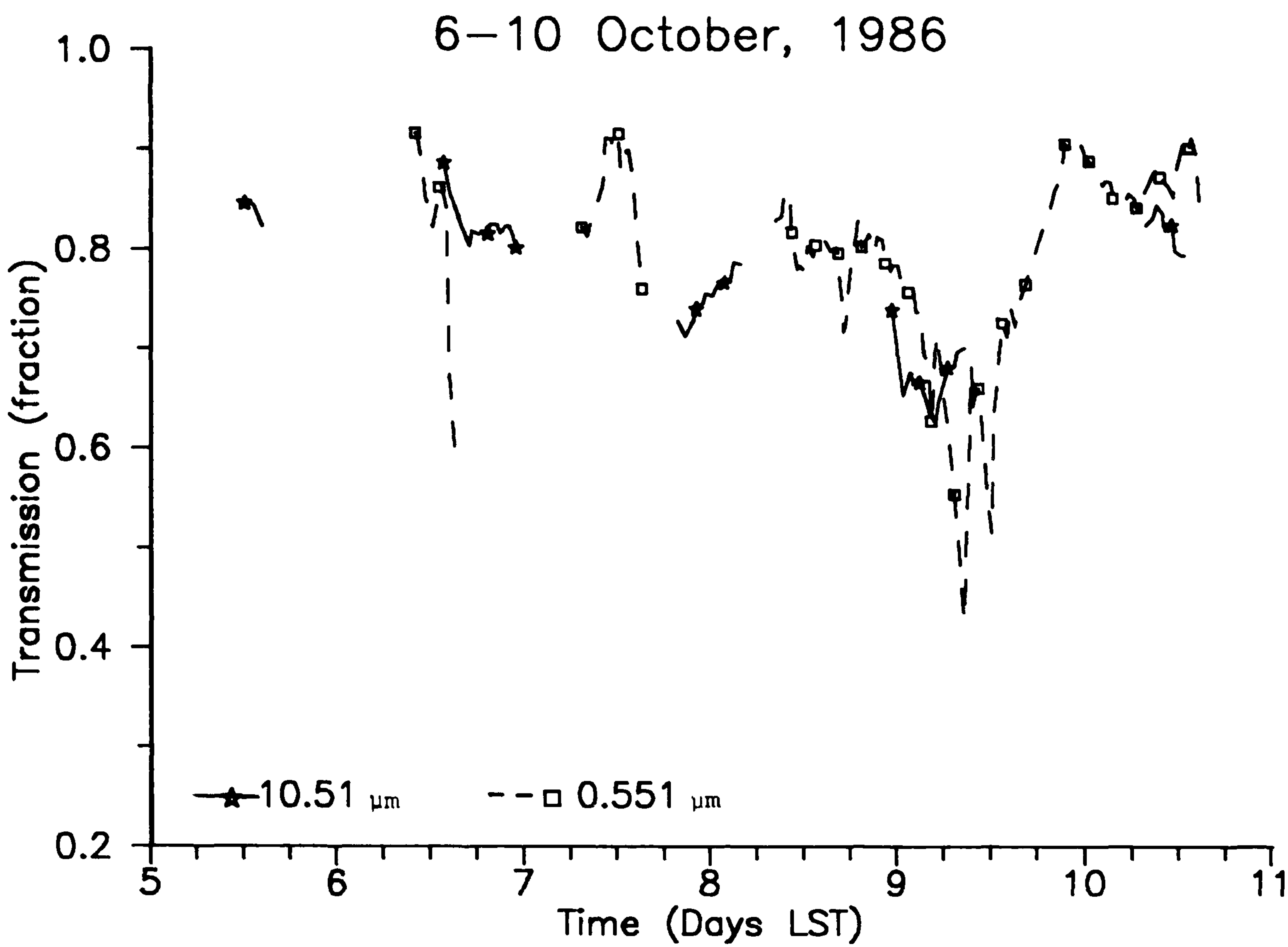

Figure 11. Transmission at 0.551 and 10.51 µm as a Function of Time for the Period 6-10 October 1986

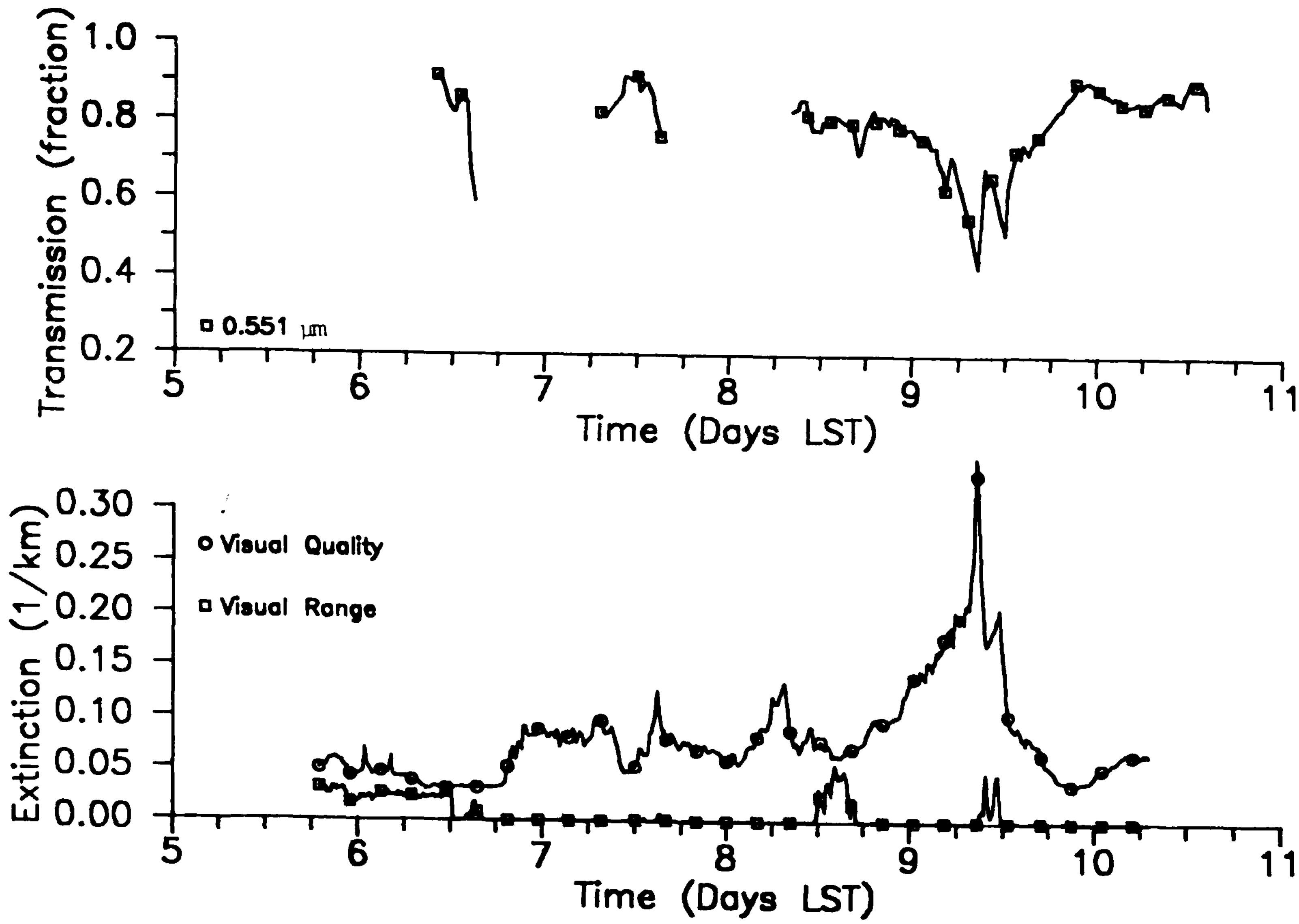

Figure 12. Visual Quality and Visual Range Data as a Function of Time for the Period 6-10 October 1986. Transmission Data at 0.551 µm are Shown for Comparison Purposes

lower values about the same time as the relative humidity values.

3.4.2 Visual Range

The visual range extinction data were generally zero throughout the tests except for selected periods of time. The non-zero values on late 5 October and on early 6 October may be associated with the frontal passage that occurred during that time period. Wind speeds had picked up (e.g. Figure 3 (c.)) and may have loaded the air with large particles that the Wright & Wright instrument could detect. The non-zero values on 8 October also occurred during a period of higher wind speeds and may also represent additional loading of particulates. The period on 9 October is most likely associated with the reported fog.

3.5 Aerosol Data

3.5.1 Size Distributions

One of the goals of this study was to determine the representative size distributions for the aerosols at the test sites. It was difficult to construct size distributions from the raw PMS aerosol data because of the overlapping of size ranges and because data were often missing from size bins. Instead, the data were handled by fitting a least-squares straight line through the log-log plots of the available data. Using the slopes and intercepts obtained from the least-squares fit, a size distribution was determined for each set of PMS data for a particular time period. Figure 13 (a.) - (d.) show the resulting daily averaged size distributions resulting from the least-squares fitting. Figure 14 (a.) and (b.) show the slopes and intercepts, respectively, as a function of time for the test period. The resultant slopes are comparable to those for a Junge distribution for atmospheric aerosols[3]. Pruppacher and Klett[4] quote similar values.

One can crudely compare these to the AFGL aerosol models[5]. The boundary layer aerosol size distributions are represented by a bimodal log normal distribution. Over the radius range 0.1 to 1.0 μm, a line with a slope of -4.6 could be used to approximate the size distribution, while over the range 1.0 to about 20.0 μm, a line with a slope of -3.6 could be used. The latter results are, to a first order, consistent with those obtained from the FTD aerosols data set. One must keep in mind, however, that the analysis performed on the FTD aerosol data set has been limited. A more detailed analysis could be performed to obtain a set of log normal parameters for the size distribution.

3. Junge, C. E., (1963) Air Chemistry and Radioactivity, Academic Press, New York, New York.
4. Pruppacher, H. and Klett, J. D. (1980) Microphysics of Clouds and Precipitation, D. Reidel Publishing Company, Dordrecht, Holland.
5. Shettle, E. P. and Fenn, R. W. (1979) Models for the Aerosols of the Lower Atmosphere and the Effects of Humidity on their Optical Properties, Air Force Geophysics Laboratory, Hanscom AFB, Massachusetts, AFGL-TR-79-0214, 20 September 1979. ADA085951

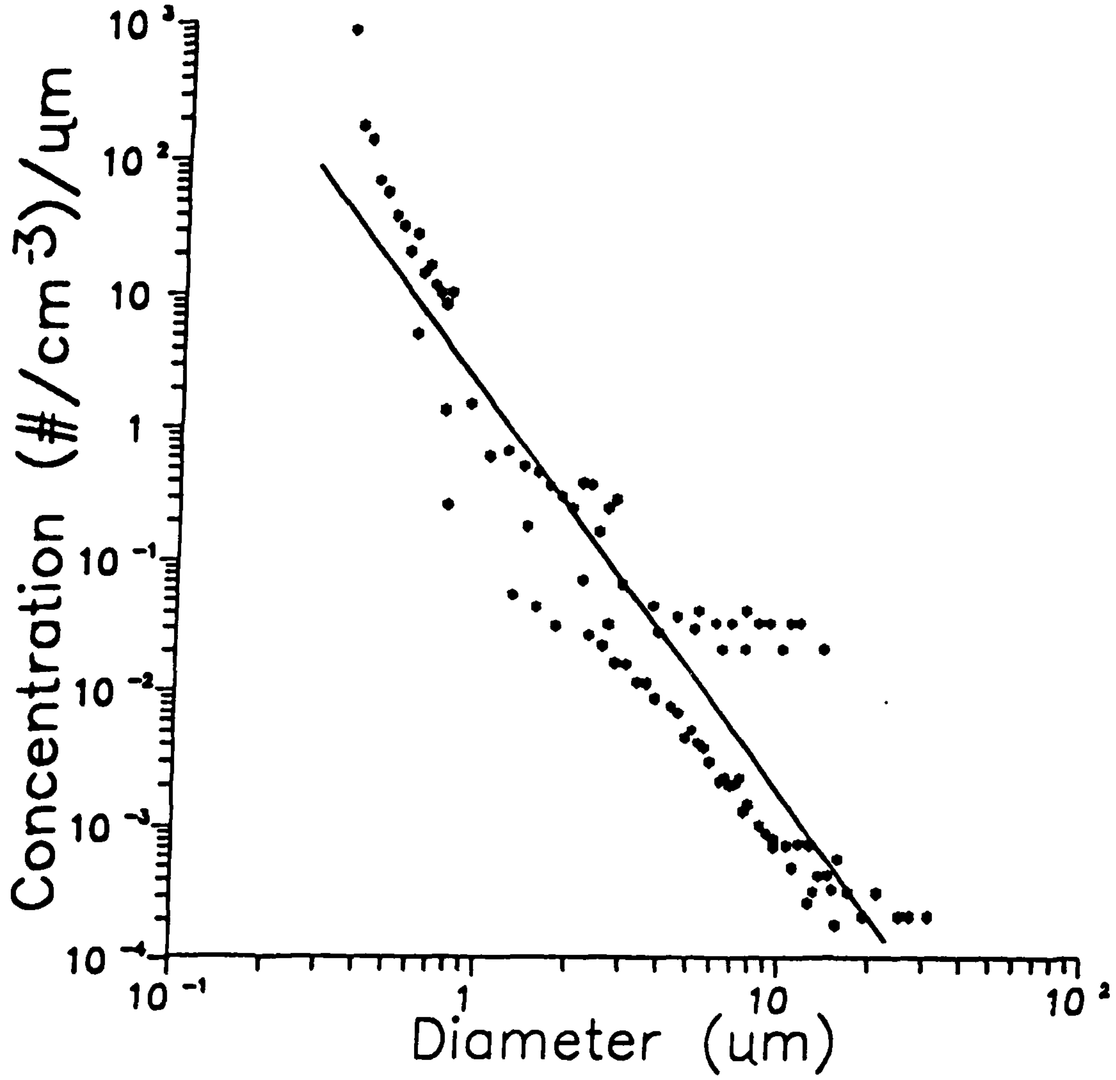

Figure 13. (a.) Daily Average Size Distribution for 6 October 1986. The Data are Fitted with the Curve 1.70 $d^{-3.01}$

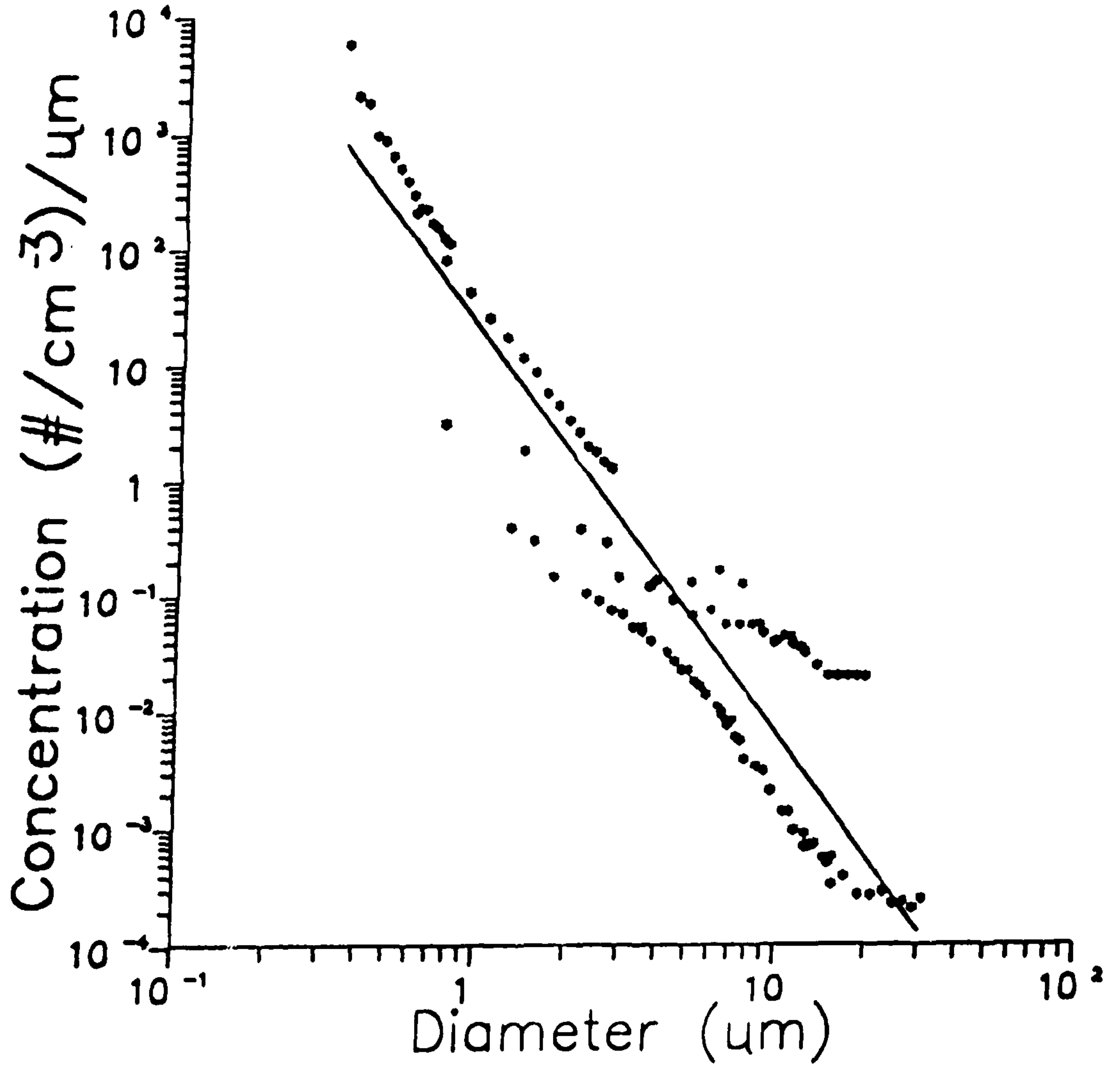

Figure 13. (b.) Daily Average Size Distribution for 7 October 1986. The Data are Fitted with the Curve 19.13 $d^{-3.46}$

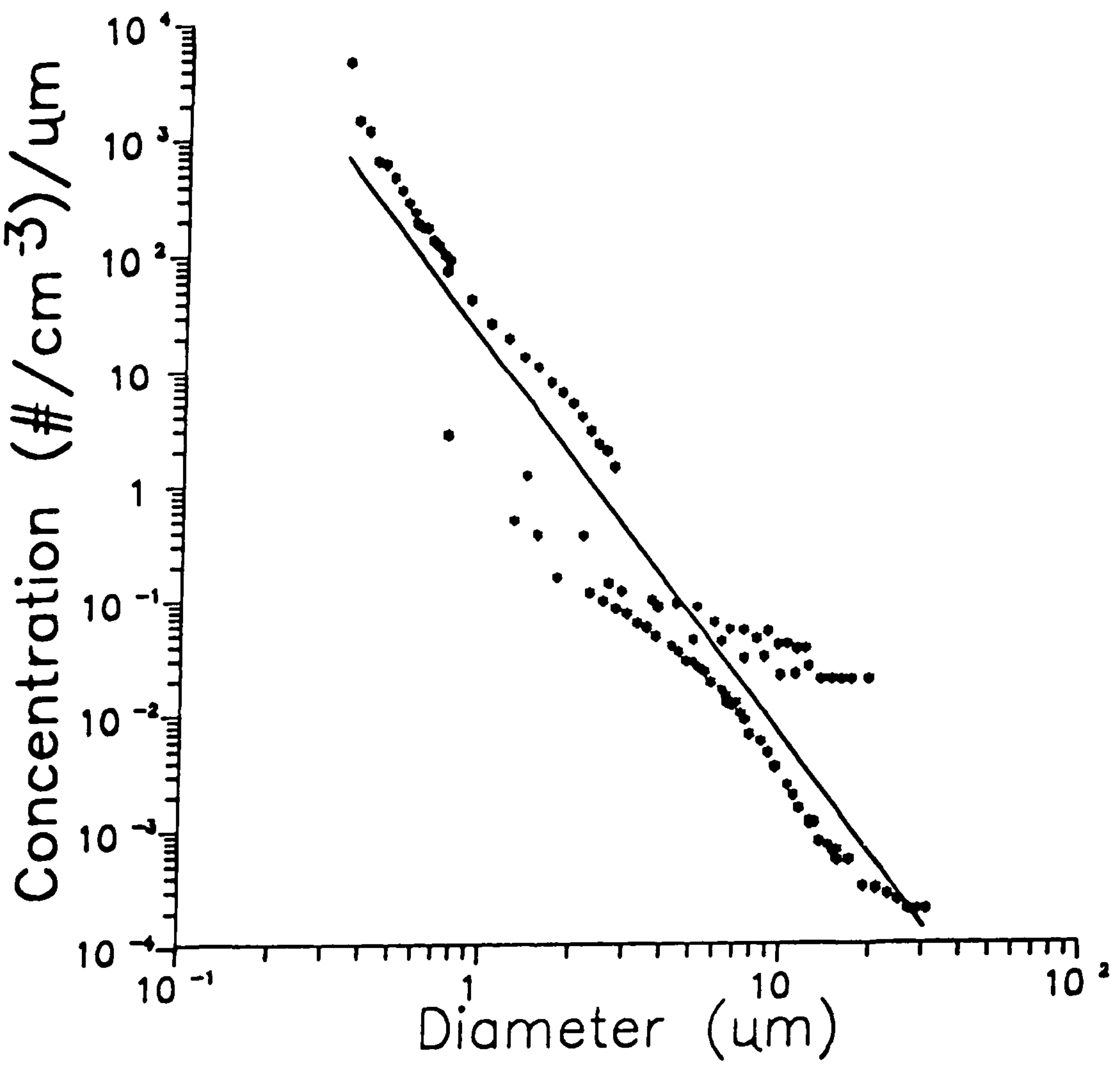

Figure 13. (c.) Daily Average Size Distribution for 8 October 1986. The Data are Fitted with the Curve 17.8 $d^{-3.42}$

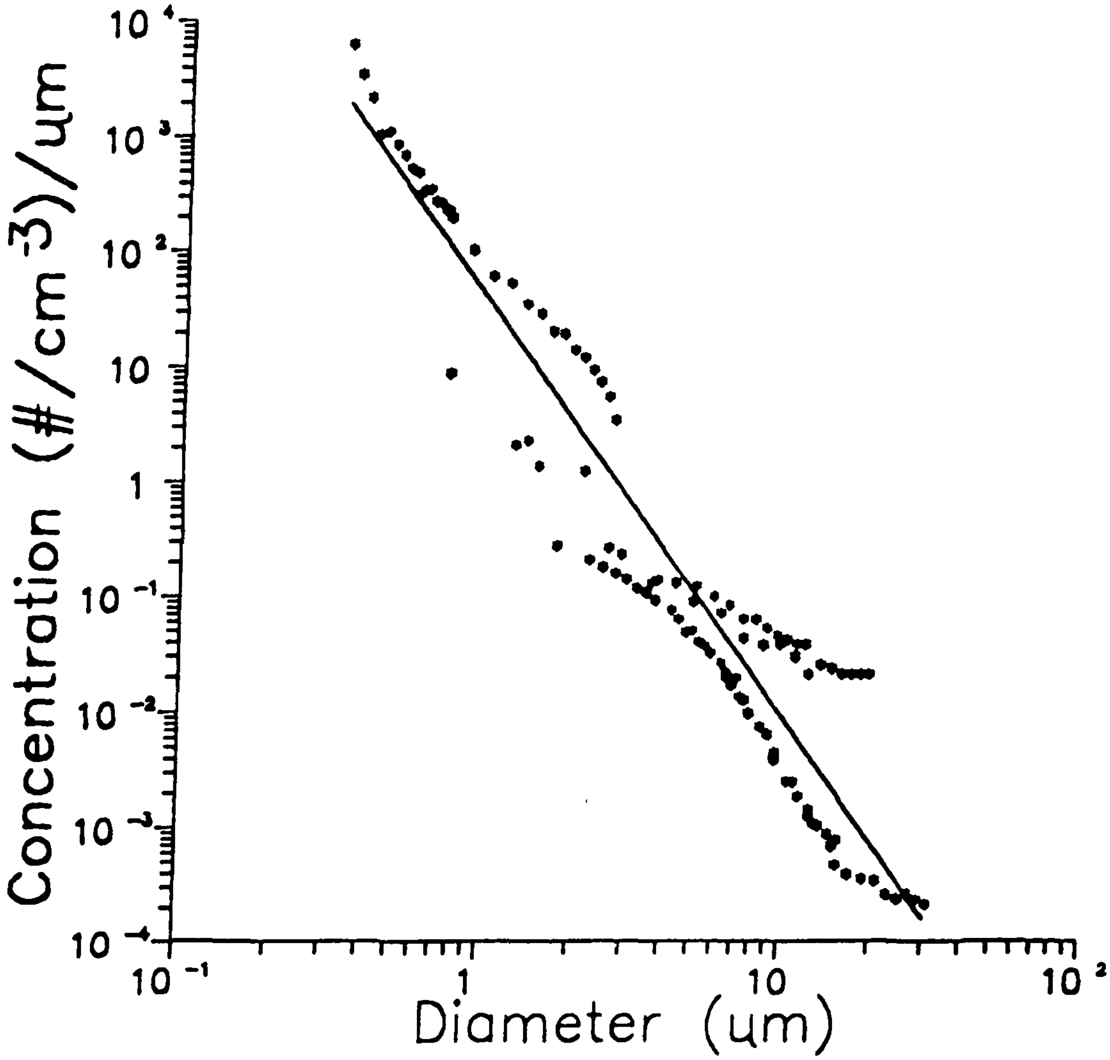

Figure 13. (d.) Daily Average Size Distribution for 9 October 1986. The Data are Fitted with the Curve 37.5 $d^{-3.62}$

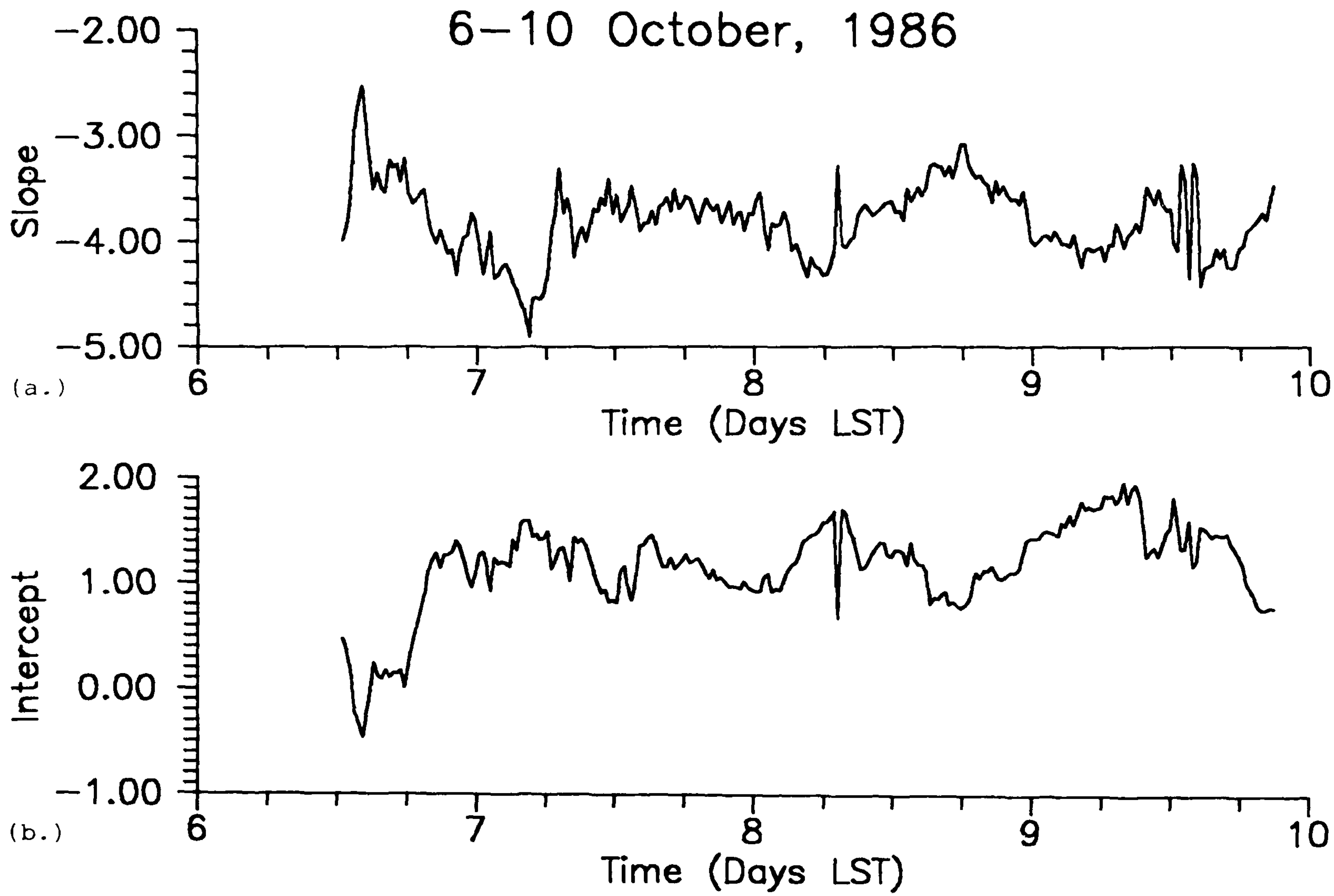

Figure 14. (a.) Slopes and (b.) Intercepts as a Function of Time for the Fitted Aerosol Size Distributions

3.5.2 Statistical Parameters

The variations in the aerosols have been studied through the use of the following statistical parameters[6]:

- the geometric mean diameter
- the geometric standard deviation of the logarithms of the diameters
- the diameter of the average volume
- the volume mean diameter
- the aerosol number concentration
- the second moment sum
- the third moment sum

The formulae for all of the above parameters are presented in the Appendix, and Figures 15 (a.) - (d.) display the results.

The geometric mean diameter, standard deviation of the logarithms of the diameter, diameter of the average volume and volume mean diameter are all in-phase with one another, and out-of-phase with the aerosol concentration. The conclusion to draw from this is that when concentration increases it does so on the small end of the particle spectrum.

The aerosol data for about 0700 LST on 8 October should not be believed. The aerosol concentration dropped to nearly zero and rebounded quickly. An examination of the raw data file indicated that the FSSP probe was not operating during the time period in question.

6. Hines, W. C. (1982) Aerosol Technology: Properties, Behavior and Measurement of Airborne Particles, John Wiley & Sons, New York, pp. 69-97.

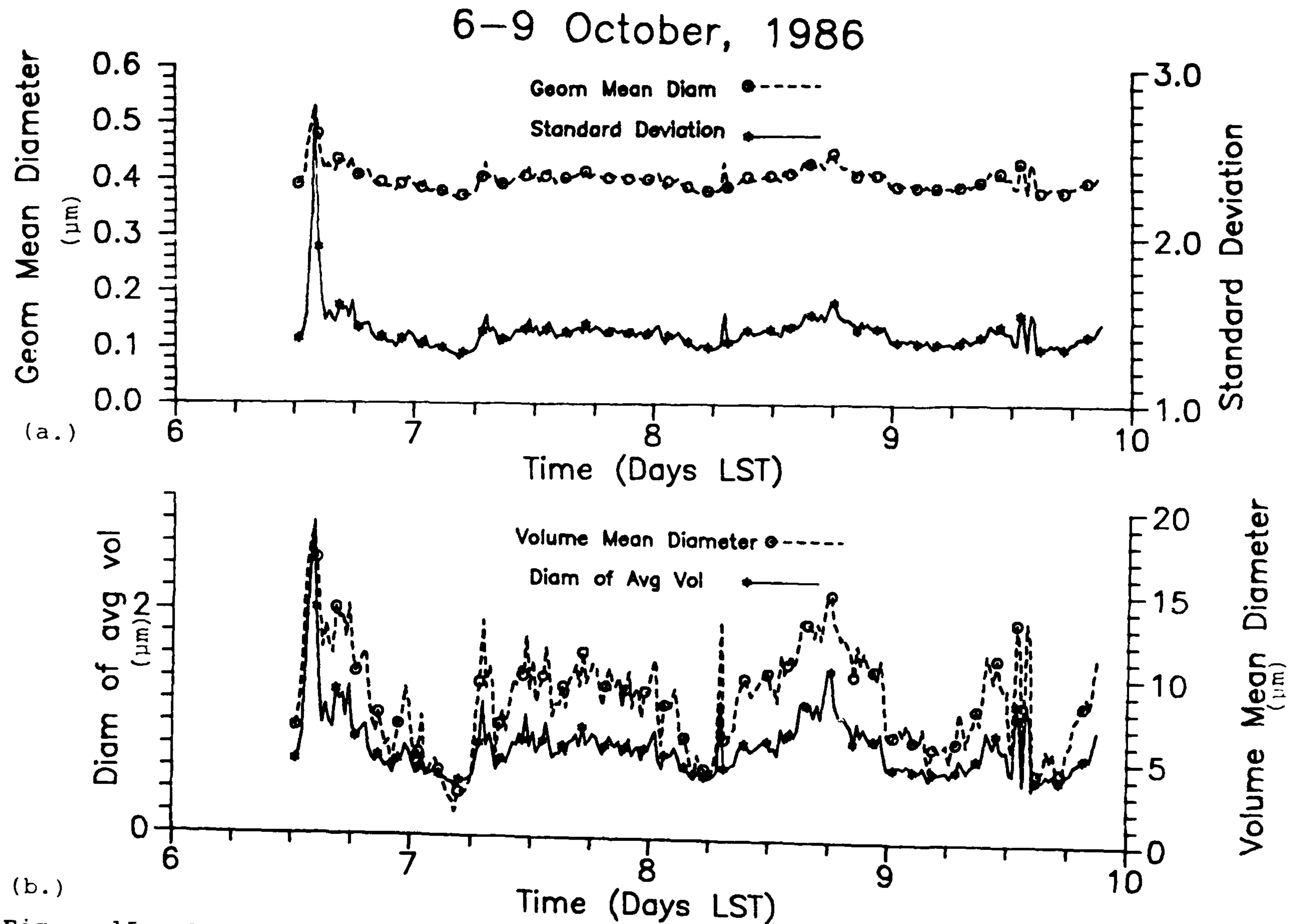

Figure 15. Aerosol Statistical Parameters for the Period 6 - 9 October 1986: (a.) Geometric Mean Diameter and Standard Deviation of the Logarithms, (b.) Volume Mean Diameter and Diameter of the Average Volume

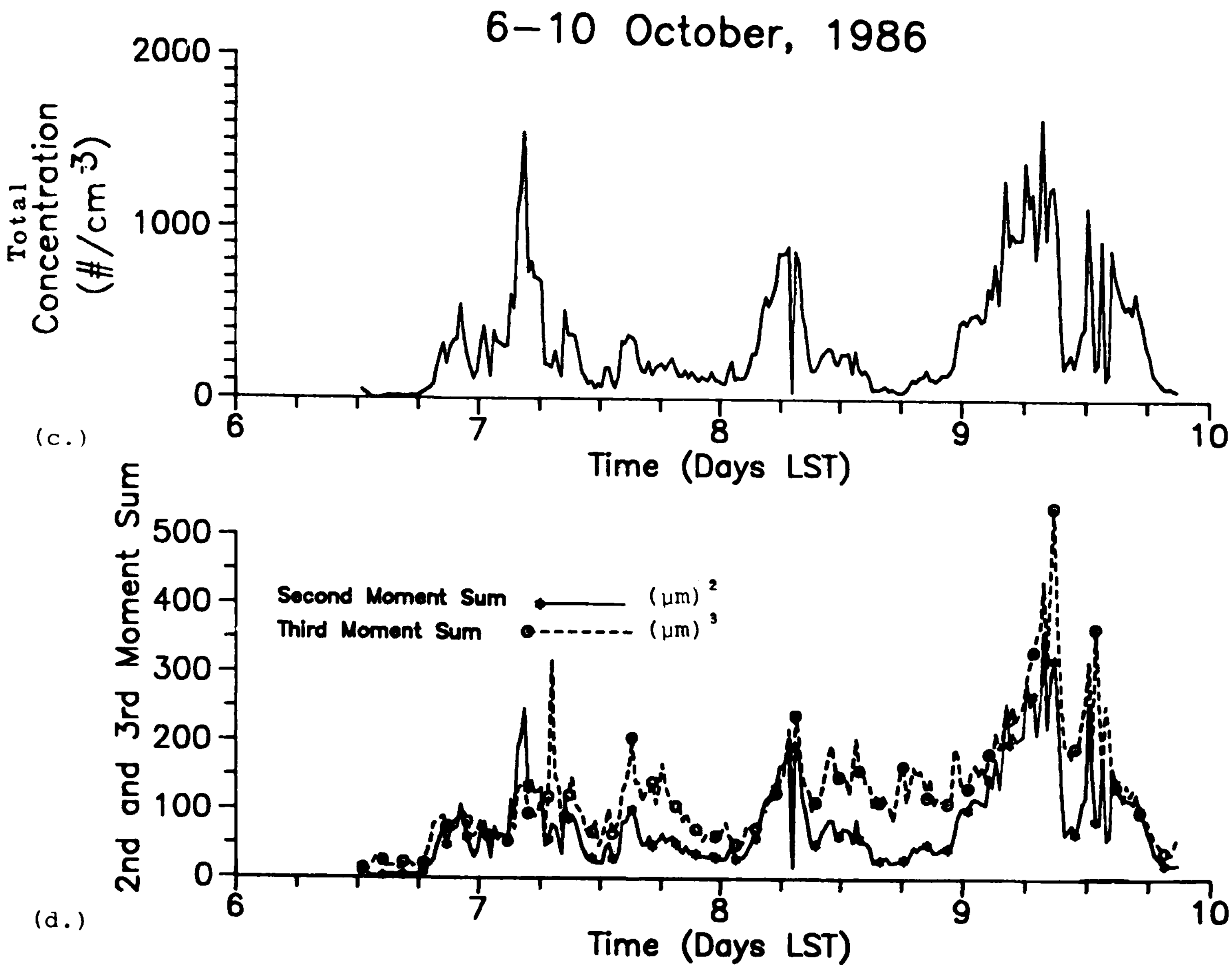

Figure 15. Aerosol Statistical Parameters for the Period 6 - 9 October 1986: (c.) Concentration and (d.) Second and Third Moment Sums.

The second and third moment sums behave in an interesting fashion. As seen in Figure 15 (d.), the general trend is for the two parameters to track one another with the third moment sum exceeding the second moment sum. However, during the time period 0000 - 0600 LST for each day of the tests, the second and third moment sums are nearly equal indicating that the particles were tending to be small, 1.0μ m or less in diameter.

3.5.3 Comparison of the PMS Data Set With EMACS Data

There is a diurnal cycle in the aerosol concentration data that may be deceptive. The concentrations generally reach a maximum in the early morning, around 0300 - 0800 LST. This is approximately the same time the relative humidities are maximum (e.g. Figure 3 (b.)) and the wind speeds are minimum (e.g. Figure 3 (c.)).

The observation that the wind speeds are at a minimum suggest that additional aerosols are not being transported in or being stirred up from the surface. The observation that the relative humidities are at a maximum suggests hygroscopic processes at work and that the existing aerosols are increasing in size to the point where the PMS equipment can begin to detect them. The results of Shettle and Fenn[5] indicate that the particle concentrations at the smallest detectable size for the PMS can vary as much as a factor of two for the changes in relative humidity that are occurring during this time period. Therefore, we conclude that more particles are large enough to be detected rather than more particles being generated or transported into the area.

Wind direction appears to have played a lesser role in the variation of particle concentration. This is surprising due to the number of potential pollution sources. The test site is located to the east of Dayton and there is a cement plant located to the northwest. Under north-northwest winds on 6 October, aerosol concentrations were quite low. On 9 October, the day of a frontal passage, winds shifted to north-northeast and particle concentrations went through strong oscillations, with concentrations decreasing to low levels by evening. When winds were from the south-southwest, such as on 7 and 8 October, concentrations were low. Thus, there is no strong evidence to support a preferred wind direction for high particle concentrations.

Particle concentrations and visual quality were generally directly related in that as particle concentrations increased, so did the visual quality data. There is one time period however, in which this relationship appeared to breakdown.

On 7 October between about 0300-0600 LST, the particle concentration increased from about 300 to 1600 cm^{-3}. During the same time period, the visual quality data were nearly constant at about 0.1 km^{-1}. The slope of the least squares fit was the steepest during this time period, indicating a size distribution with reduced numbers of large particles.

These conclusions are also demonstrated in the other statistical parameters shown in Figure 15.

3.6 Aerosol Angular Scattering Data

The APN data were, in general, of questionable quality. The standard deviations were often of the same magnitude as the average values and sometimes were larger. Negative values were also often reported from modules 1 and 2 and indicate a calibration problem with the instrument. The data from module 3 were given as uncalibrated, digital signal counts and need to be reduced before they can be used.

As noted in Table 5, APN data were available on 2, 4, 5 and 9 October. Only on 9 October was there any companion meteorological or transmission data. APN data were available for three time periods and these data are shown in Figures 16 (a.) - (c.).

Of the three time periods from 9 October, 0515 - 0620 LST was the one with the highest visual quality and lowest transmission values (e.g. Figure 12). The module 1 APN data were also generally highest during this period.

It was hoped that the APN data could be used to provide some information about the character, or type of the aerosols being studied. Unfortunately, the data could not be used for that purpose. Ratios of the module 1 data at the three scattering angles were evaluated. These ratios were compared against ratios of the aerosol phase functions, at

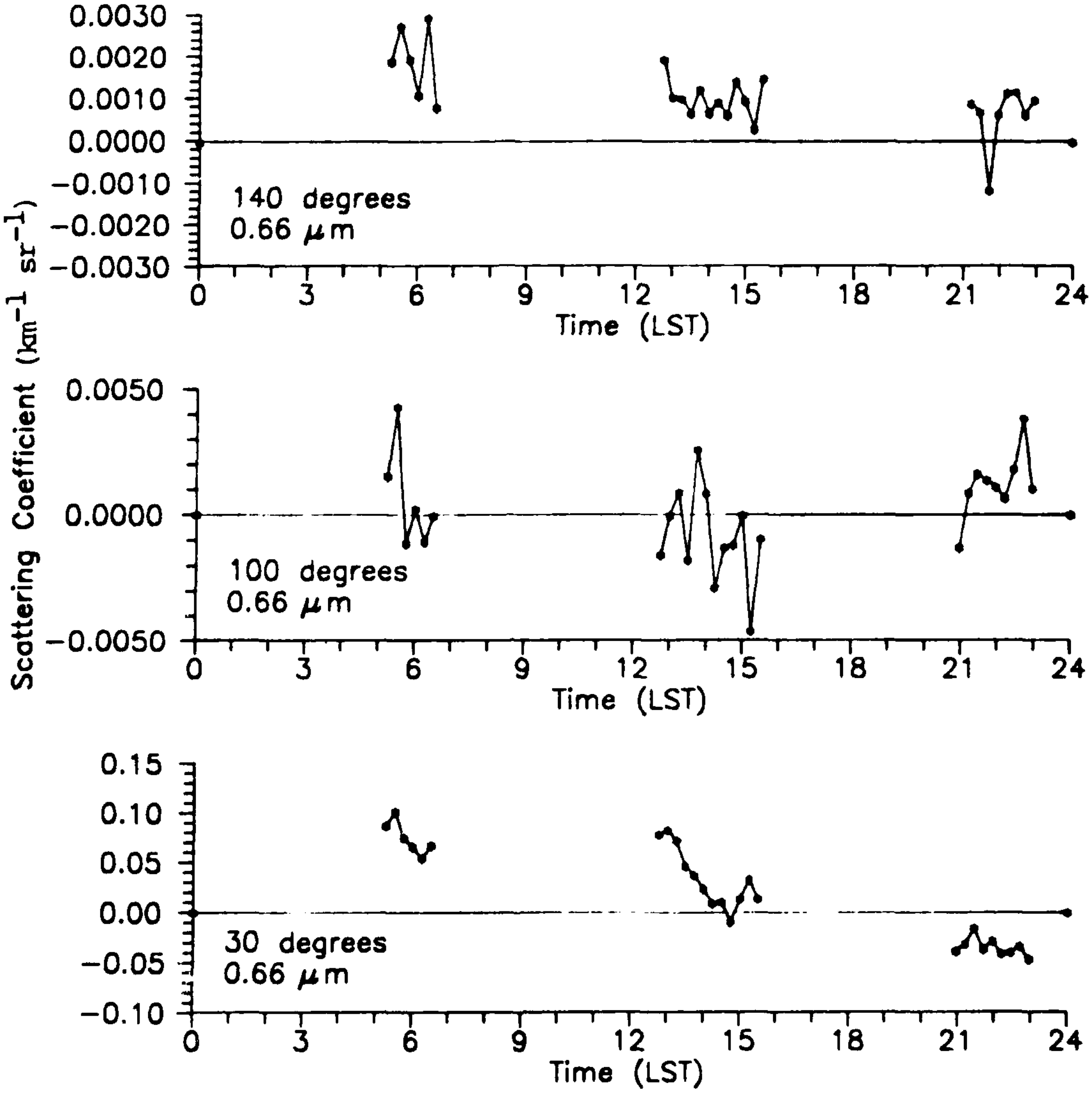

Figure 16. APN Data for 9 October 1986 for (a.) Module 1, 0.66 μm

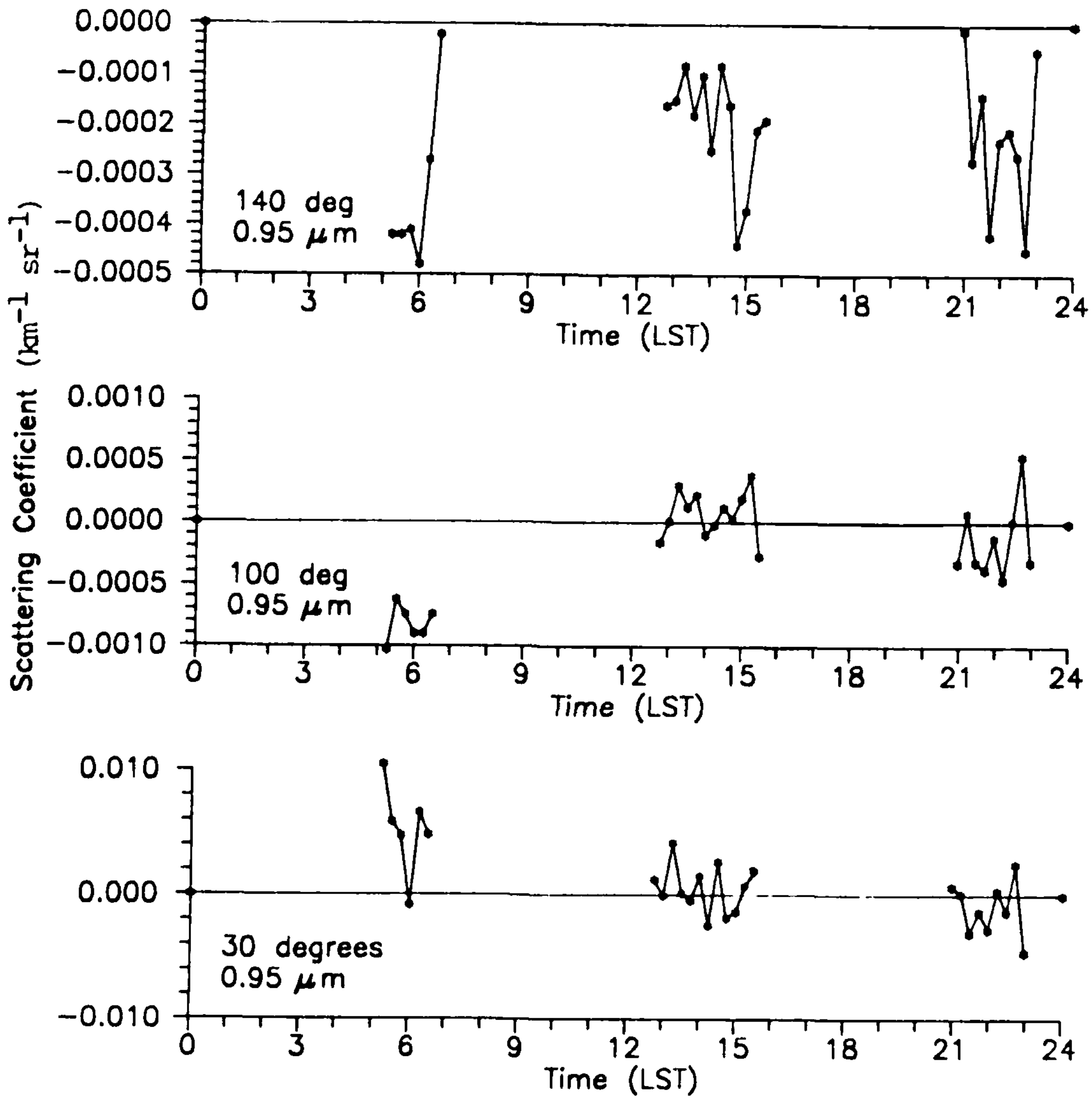

Figure 16. APN Data for 9 October 1986 for (b.) Module 2, 0.95 μm

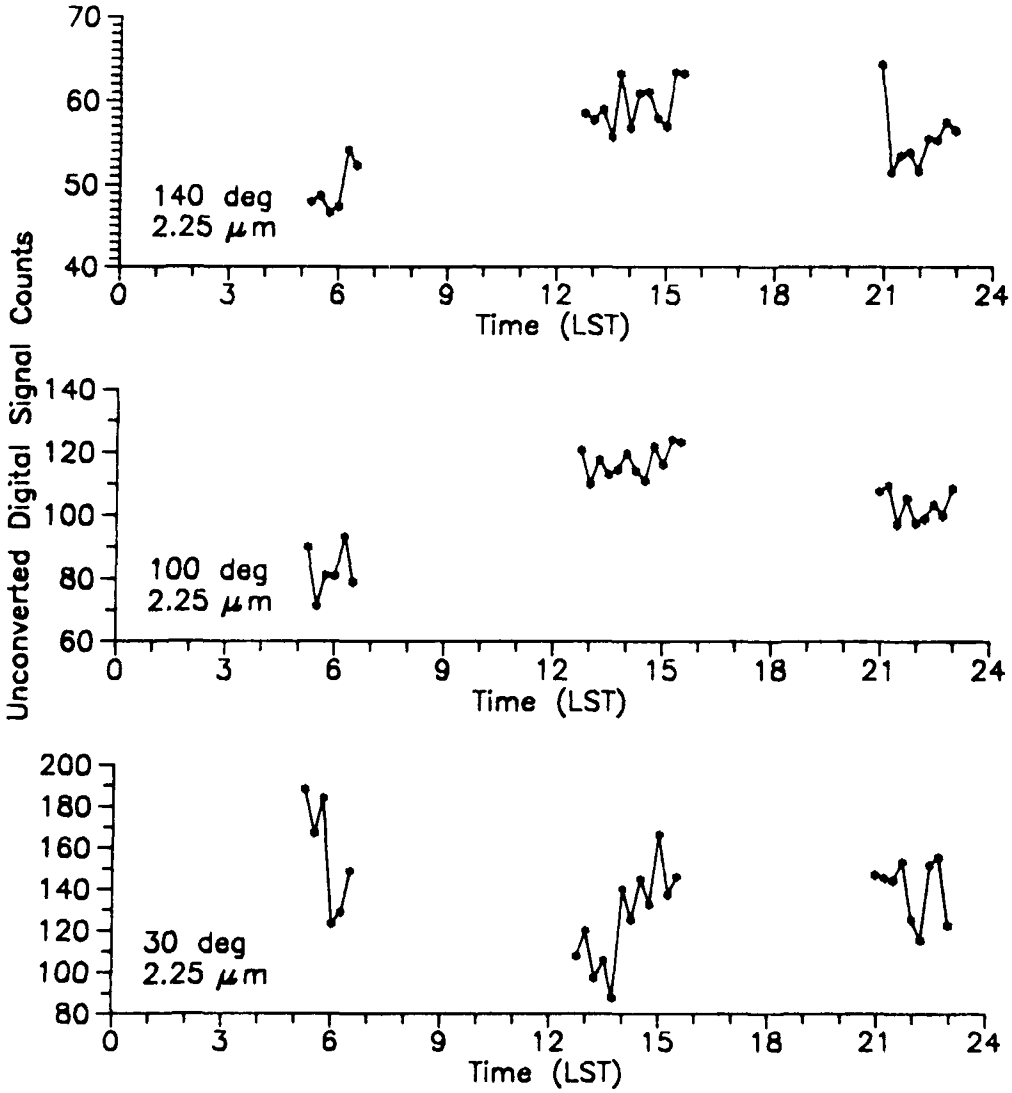

Figure 16. APN Data for 9 October 1986 for (c.) Module 3, 2.25 μm

at the same scattering angles, of the AFGL aerosol models currently used (Shettle, private communication). The ratio of the 30° to 100° APN data ranged from 16 to 70 while that for the 30° to 140° data ranged from 11 to 300. From one time period to another, the variations in these ratios was as large as a factor of 5. For relative humidities similar to those on 9 October, the ratios of the AFGL aerosol model phase functions ranged from 16 to 35. In other words, the ratios of the APN data encompassed all of the possible AFGL aerosol models and could not be used to characterize the type of aerosols present. (The ratios of the APN data, in fact, encompassed the range of values for all of the AFGL aerosol models at any relative humidity.) This was also true when comparing the module 1 and 2 data at 30°. The ratio of the module 1 to module 2 data ranged from 7 to 20 while ratios evaluated for the AFGL aerosol models at similar wavelengths were about 1.

4. SUMMARY AND CONCLUSIONS

The purpose of this project was to review, validate and analyze data taken in support of operations to study the scattering and extinction properties of atmospheric particulates. Various types of environmental, transmission and particulate data were taken in order to achieve the desired goal. The review of the data revealed some problems and inconsistencies that made a complete analysis difficult.

4.1 Meteorological Data

The meteorological data taken by the EMACS appear to be reasonable. The data agree with the routine surface weather observations taken by the AWS observers.

4.2 Transmission Data

The transmission data are highly suspect, especially in the infrared. No explanation can be provided to the inconsistencies and problems that have been observed. They may be due to problems in the transmissometer, but without full documentation on test procedures, instrument problems encountered, etc. one can only speculate.

The visible transmission data qualitatively agree with the environmental data and change with respect to atmospheric moisture as would be expected. The visible transmission data also qualitatively agree with the visual quality data. The data from 6 October exhibit an unexplained sudden drop in transmission in the visible and the near IR wavelengths that is not mirrored in any of the environmental data. It is suspected that there were problems with the transmissometer on that day.

The infrared transmission data especially suffer from inconsistencies. On 6 October, the data are significantly lower than expected and on 7 October, the data at 10.51 μm track inversely to the visible and near IR data.

4.3 Visual Quality and Visual Range Data

The visual quality data qualitatively agree with the visibility observations taken by the AWS observers. While the magnitudes cannot be accurately compared, the changes in visibility reported by AWS are reflected in the visual quality data. A weak diurnal signal that can be related to diurnal variations in the relative humidity can also be seen.

The visual range data were generally zero throughout the tests. The non-zero values corresponded with time periods when large aerosol particles, for which the visual range equipment was designed, could have been present.

4.4 Aerosol Data

Particle concentration and the second and third moment sums appeared to be in phase with one another. The magnitudes of the peaks of the moment sums was dependent on the size distribution. A change to higher numbers of particles below 1 μm made the size distribution steeper and caused the second moment sum value to approach and sometimes exceed the third moment sum.

The geometric mean diameter, mass mean diameter and diameter of the average volume all tracked one another, and tracked opposite the particle concentration. This meant that the mean diameters were getting smaller as particle concentration increased and vice versa. Particles were being added at the small end of the distribution when concentrations increased, and were taken out of the smaller end when concentrations decreased.

Particle concentrations showed no preference towards wind direction, despite the presence of a large city with its associated sources of pollution to the west. Particle concentrations seemed to be primarily forced by the amount of mixing that is occurring.

4.5 Angular Scattering Data

An important part of these tests was the performance of the prototype APN instrument. Limited data were available from the instrument and only on one day, 9 October, was there any companion data from any of the other instruments.

The data from the APN were, in general, of questionable quality. The standard deviations were often of the same magnitude or larger than the average values. Negative values were often also reported from module 1 (0.66 μm) and module 2 (0.95 μm). These occurrences of negative values generally correlated with periods of high visibility and most likely represent the noise in the instrument. Module 3 (2.25 μm) yielded data given as uncalibrated, digital signal counts.

It was hoped that the APN data could be used to provide some information about the character, or type, of the aerosols being studied. Unfortunately, the data could not be used for that purpose. Ratios of the module 1 data at the three scattering angles were evaluated and compared against similar ratios for the AFGL aerosol models. The ratios of the APN data varied widely from one time period to another and encompassed the ratios of all of the AFGL aerosol models at all relative humidities. A similar analysis was performed involving ratios of the module 1 and module 2 data at 30° scattering angle. There was no agreement between these results and similar calculations for the AFGL aerosol models.

References

1. Kneizys, F. X., Gruenzel, R. R., Martin, W. C., Schuwerk, M. J., Gallery, W. O., Clough, S. A., Chetwynd, Jr., J. H., and Shettle, E. P. (1984) Comparisons of 8 to 12 Micrometer and 3 to 5 Micrometer CVF Transmissometer Data with LOWTRAN Calculations, Air Force Geophysics Laboratory, Hanscom AFB, Massachusetts, AFGL-TR-84-0171, 26 June 1984, ADA154218.

2. Climate Analysis Center (1986) Daily Weather Maps, Weekly Series 6-12 October 1986, National Oceanic and Atmospheric Administration, Washington, D. C.

3. Junge, C. E., (1963) Air Chemistry and Radioactivity, Academic Press, New York, New York.

4. Pruppacher, H. and Klett, J. D. (1980) Microphysics of Clouds and Precipitation , D. Reidel Publishing Company, Dordrecht, Holland.

5. Shettle, E. P. and Fenn, R. W. (1979) Models for the Aerosols of the Lower Atmosphere and the Effects of Humidity on their Optical Properties, Air Force Geophysics Laboratory, Hanscom AFB, Massachusetts, AFGL-TR-79-0214, 20 September 1979, ADA085951.

6. Hines, W. C. (1982) Aerosol Technology: Properties, Behavior and Measurement of Airborne Particles, John Wiley & Sons, New York, pp. 69-97.

Appendix A

Formula for the Calculation of Aerosol Parameters

Each aerosol data record consisted of a number that corresponded to a particular size bin and a second number that was the number density of particles counted in the bin divided by the width of the bin. From these data, a number of parameters related to aerosol properties can be calculated.

A.1 Total Particle Concentration

The total particle concentration, N, in # cm^{-3} is given by

$$N = \sum_{i=1}^{m} n_i \, d_i$$

where n_i is the number of particles in bin i divided by the bin width, d_i is the midpoint diameter of the bin size and m is the total number of bins. The midpoint diameter of the size bin is given by

$$d_i = (d_{i'high} - d_{i'low})/2$$

where $d_{i'high}$ and $d_{i,low}$ are the upper and lower particle diameters covered by size bin i.

A.2 Lognormal Size Distribution Parameters

Lognormal size distributions, a normal distribution of the logarithms of the particle sizes, are commonly used to describe aerosol size distributions. There is no theoretical basis for this kind of distribution but they are used because they generally fit the wide range and skewed shapes of actual aerosol size distributions. Two parameters are needed to describe the lognormal distribution, the geometric mean diameter and the geometric standard deviation.

The geometric mean diameter, d_g, is given by

$$d_g = \exp\left[\frac{\sum_{i=0}^{m} n_i \log (d_i)}{N}\right]$$

The geometric standard deviation, σ_g, is given by

$$\log (\sigma_g) = \left[\frac{\sum_{i=0}^{m} n_i (\log (d_i)-\log (d_g))^2}{(N-1)}\right]^{1/2}$$

A.3 Statistical Parameters

A.3.1 Diameter of the Average Volume

The diameter of the average volume, d_{av}, is evaluated on the basis of the total number of particles present and is given by

$$d_{av} = \left[\sum_{i=1}^{m} n_i (d_i)^3 / N\right]^{1/3}$$

This quantity is also called the third moment average. Also, if one assumes sperical particles and a constant density for the aerosols, this quantity is equivalent to the diameter of the average mass.

A.3.2 Volume Mean Diameter

The volume mean diameter, d_{mv}, is evaluated by weighting the volume of the particles in bin size d_i against the total volume of all of the particles. The expression is given as

$$d_{mv} = \frac{\sum_{i=1}^{m} n_i \, (d_i)^4}{\sum_{i=1}^{m} n_i \, (d_i)^3}$$

If one assumes spherical particles and a constant density for the aerosols, d_{mv} is equivalent to the mass mean diameter.

A.4 Moment Sums

Moment sums are related to moment averages and the power associated with the moment (second, third, ...) allows one to evaluate aerosol properties in terms of quantities such as surface area and volume or mass. The second moment sum, M_2, is proportional to the total scattering area and is given by

$$M_2 = \sum_{i=1}^{m} n_i (d_i)^2$$

The third moment sum, M_3, is proportional to the total volume of the aerosol sample and is given by

$$M_3 = \sum_{i=1}^{m} n_i (d_i)^3$$